

Romain PINQUIE

MSc Computer Aided Engineering

CAE

Advanced

Applications

Assignment Report

30/03/2012

SUMMARY

I. INTRODUCTION	5
II. OVERVIEW OF THE PROBLEM	5
1. What is the objective?	5
2. What is known?	5
A. Geometry	5
B. Material	7
C. Vehicle load	7
3. Three case studies	7
A. Free wing	7
B. Free wing and outboard flange stiffener	7
C. Free wing and stiffeners along the flange and web	8
III. CALCULATIONS AND ASSUMPTIONS	8
1. Rail assumptions	8
2. Web and Flange assumptions	9
3. Turret assumptions	9
4. Load	10
IV. 1ST CASE STUDY: FREE WING	10
1. Scheme	10
2. Geometries	10
A. Shell & Beam elements Models	10
B. Shell elements Models	11
3. Load & Boundary conditions	11
A. Load	11
B. Boundary conditions	11
4. Free Mesh	12
A. Mesh & Elements formulation	12
B. Post-processing	13
5. Mesh	14
A. Partitioning of the structures	14
B. Convergence	15
6. Models – Elements formulation	17

7. Post-processing.....	18
A. Equilibrium	18
B. Shell post-processing	19
C. Stress post-processing	20
D. Displacements post-processing.....	23
V. 2ND CASE STUDY: FREE WING + FLANGE STIFFENER.....	25
1. Geometry	25
2. Load & Boundary conditions	25
3. Mesh & Elements	26
4. Models	26
5. Post-processing.....	27
A. Equilibrium	27
B. Shell post-processing	27
C. Von-Mises stress contours	28
D. Displacements contours	30
VI. 3RD CASE STUDY: FREE WING + FLANGE & WEB STIFFENERS	32
1. Geometry	32
2. Load & Boundary conditions	32
3. Mesh & Elements	33
4. Models	33
5. Post-processing.....	34
A. Stress post-processing	34
B. Displacements post-processing.....	36
VII. CONCLUSION.....	38

Table of Figures

<i>FIGURE 1 - SIMPLIFIED REPRESENTATION OF THE FRONT INNER WING ASSEMBLY OF A CAR</i>	6
<i>FIGURE 2 - 1ST CASE STUDY: FREE WING</i>	6
<i>FIGURE 3 - DETAIL OF TURRET CAP</i>	7
<i>FIGURE 4 - 2ND CASE STUDY: FREE WING + FLANGE STIFFENER</i>	8
<i>FIGURE 5 - 3RD CASE STUDY: FREE WING + FLANGE & WEB STIFFENERS</i>	8
<i>FIGURE 6 - BEAM'S PROPERTIES</i>	9
<i>FIGURE 7 - 1ST CASE STUDY: FREE WING MODEL</i>	10
<i>FIGURE 8 - GEOMETRY FOR BEAM & SHELL ELEMENTS MODELS</i>	10
<i>FIGURE 9 - GEOMETRY FOR SHELL ELEMENTS MODEL</i>	11
<i>FIGURE 10 - PRESSURE LOAD 0.191 N/MM²</i>	11
<i>FIGURE 11 - BCs FOR BEAM & SHELL ELEMENTS MODELS</i>	12
<i>FIGURE 12 - BCs FOR SHELL ELEMENTS MODELS</i>	12
<i>FIGURE 13 - FREE MESH USING S4R & B31</i>	12
<i>FIGURE 14 - FREE MESH USING S4R</i>	12
<i>FIGURE 15 - VON-MISES STRESS FOR B31 & S4R</i>	13
<i>FIGURE 16 - VON-MISES STRESS FOR S4R</i>	13
<i>FIGURE 17 - DEFLECTION ALONG THE VERTICAL AXIS FOR B31 & S4R</i>	14
<i>FIGURE 18 - DEFLECTION ALONG THE VERTICAL AXIS FOR S4R</i>	14
<i>FIGURE 19 - FREE WING WITH PARTITIONS (BEAM & SHELL MODELS)</i>	15
<i>FIGURE 20 - FREE WING WITH PARTITIONS (SHELL MODELS)</i>	15
<i>FIGURE 21 - FREE WING, SIZE 50, USING B31 & S4R</i>	15
<i>FIGURE 22 - FREE WING, SIZE 40, USING B31 & S4R</i>	15
<i>FIGURE 23 - FREE WING, SIZE 30, USING B31 & S4R</i>	16
<i>FIGURE 24 - FREE WING, SIZE 20, USING B31 & S4R</i>	16
<i>FIGURE 25 - CONVERGENCE OF THE MAXIMUM DEFLECTION</i>	16
<i>FIGURE 26 - CONVERGENCE OF THE VON-MISES STRESS</i>	17
<i>FIGURE 27 - EQUILIBRIUM STUDY FOR THE FREE WING</i>	18
<i>FIGURE 28 - LOCAL SET AXIS</i>	19
<i>FIGURE 29 - MATERIAL DIRECTIONS</i>	19
<i>FIGURE 30 - SHELL DEFINITION</i>	19
<i>FIGURE 31 - VM STRESS FOR 1ST CASE STUDY (FREE WING) USING B31 & S4R</i>	20
<i>FIGURE 32 - VM STRESS FOR 1ST CASE STUDY (FREE WING) USING B31 & S4</i>	20
<i>FIGURE 33 - VM STRESS FOR 1ST CASE STUDY (FREE WING) USING B32 & S8R</i>	20
<i>FIGURE 34 - VM STRESS FOR 1ST CASE STUDY (FREE WING) USING S4R</i>	21
<i>FIGURE 35 - VM STRESS FOR 1ST CASE STUDY (FREE WING) USING S4</i>	21
<i>FIGURE 36 - MAXIMUM VON-MISES STRESS EVOLUTION FOR THE 1ST CASE STUDY (FREE WING)</i>	21
<i>FIGURE 37 - SHELL'S BEHAVIOUR EXPECTED FOR THE SHELL ELEMENTS</i>	22
<i>FIGURE 38 - SHELL ELEMENT BEHAVIOUR</i>	22
<i>FIGURE 39 - SPOS S22 STRESS FOR 1ST CASE STUDY (FREE WING) USING S4</i>	22
<i>FIGURE 40 - SNEG S22 STRESS FOR 1ST CASE STUDY (FREE WING) USING S4</i>	22
<i>FIGURE 41 - DISPLACEMENTS FOR 1ST CASE STUDY (FREE WING) USING B31 & S4R</i>	23
<i>FIGURE 42 - DISPLACEMENTS FOR 1ST CASE STUDY (FREE WING) USING B31 & S4</i>	23
<i>FIGURE 43 - DISPLACEMENTS FOR 1ST CASE STUDY (FREE WING) USING B32 & S8R</i>	23
<i>FIGURE 44 - DISPLACEMENTS FOR 1ST CASE STUDY (FREE WING) USING S4R</i>	24
<i>FIGURE 45 - DISPLACEMENTS FOR 1ST CASE STUDY (FREE WING) USING S4</i>	24
<i>FIGURE 46 - MAXIMUM DEFLECTION EVOLUTION FOR THE 1ST CASE STUDY (FREE WING)</i>	24
<i>FIGURE 47 - 2ND CASE STUDY: FREE WING + FLANGE STIFFENER</i>	25

FIGURE 48 - FLANGE STIFFENER	26
FIGURE 49 - EQUILIBRIUM STUDY FOR THE FREE WING + FLANGE STIFFENER	27
FIGURE 50 - SNEG S22 STRESS FOR 2 ND CASE STUDY (FREE WING + FLANGE STIFFENER) USING S4 & B33.....	27
FIGURE 51 - SPOS S22 STRESS FOR 2 ND CASE STUDY (FREE WING + FLANGE STIFFENER) USING S4 & B33	27
FIGURE 52 - VM STRESS FOR 2 ND CASE STUDY (FREE WING + FLANGE STIFFENER) USING B31 & S4R & B33	28
FIGURE 53 – VM STRESS FOR 2 ND CASE STUDY (FREE WING + FLANGE STIFFENER) USING B31 & S4 & B33	28
FIGURE 54 – VM STRESS FOR 2 ND CASE STUDY (FREE WING + FLANGE STIFFENER) USING B32 & S8R & B33	28
FIGURE 55 – VM STRESS FOR 2 ND CASE STUDY (FREE WING + FLANGE STIFFENER) USING S4R & B33.....	29
FIGURE 56 – VM STRESS FOR 2 ND CASE STUDY (FREE WING + FLANGE STIFFENER) USING S4 & B33.....	29
FIGURE 57 – MAXIMUM VON-MISES STRESS EVOLUTION FOR THE 2 ND CASE STUDY (FREE WING + FLANGE STIFFENER)	29
FIGURE 58 – DISPLACEMENTS FOR 2 ND CASE STUDY (FREE WING + FLANGE STIFFENER) USING B31 & S4R & B33	30
FIGURE 59 – DISPLACEMENTS FOR 2 ND CASE STUDY (FREE WING + FLANGE STIFFENER) USING B31 & S4 & B33	30
FIGURE 60 – DISPLACEMENTS FOR 2 ND CASE STUDY (FREE WING + FLANGE STIFFENER) USING B32 & S8R & B33	30
FIGURE 61 – DISPLACEMENTS FOR 2 ND CASE STUDY (FREE WING + FLANGE STIFFENER USING S4R & B33	31
FIGURE 62 – DISPLACEMENTS FOR 2 ND CASE STUDY (FREE WING + FLANGE STIFFENER) USING S4 & B33	31
FIGURE 63 – MAXIMUM DEFLECTION EVOLUTION FOR THE 2 ND CASE STUDY (FREE WING + FLANGE STIFFENER)	31
FIGURE 64 – 3 RD CASE STUDY: FREE WING + FLANGE & WEB STIFFENERS	32
FIGURE 65 - NEW PARTITIONS FOR THE 2ND CASE STUDY	32
FIGURE 66 - WEB STIFFENERS.....	33
FIGURE 67 - FINAL PART.....	33
FIGURE 70 - VM STRESS FOR 3 RD CASE STUDY (FREE WING + FLANGE & WEB STIFFENERS) USING B31 & S4R & B33	34
FIGURE 71 - VM STRESS FOR 3 RD CASE STUDY (FREE WING + FLANGE & WEB STIFFENERS) USING B31 & S4 & B33	34
FIGURE 72 - VM STRESS FOR 3 RD CASE STUDY (FREE WING + FLANGE & WEB STIFFENERS) USING B32 & S8R & B32	34
FIGURE 73 - VM STRESS FOR 3RD CASE STUDY (FREE WING + FLANGE & WEB STIFFENERS) USING S4R & B32	35
FIGURE 74 - VM STRESS FOR 3RD CASE STUDY (FREE WING + FLANGE & WEB STIFFENERS) USING S4 & B32	35
FIGURE 75 - MAXIMUM VON-MISES STRESS EVOLUTION FOR THE 3 RD CASE STUDY (FREE WING + FLANGE & WEB STIFFENERS)	35
FIGURE 76 - DISPLACEMENTS FOR 3 RD CASE STUDY (FREE WING + FLANGE & WEB STIFFENERS) USING B31 & S4R & B33	36
FIGURE 77 - DISPLACEMENTS FOR 3 RD CASE STUDY (FREE WING + FLANGE & WEB STIFFENERS) USING B31 & S4 & B33.....	36
FIGURE 78 - DISPLACEMENTS FOR 3 RD CASE STUDY (FREE WING + FLANGE & WEB STIFFENERS) USING B32 & S8R & B32	36
FIGURE 79 - DISPLACEMENTS FOR 3RD CASE STUDY (FREE WING + FLANGE & WEB STIFFENERS) USING S4R & B33	37
FIGURE 80 - DISPLACEMENTS FOR 3RD CASE STUDY (FREE WING + FLANGE & WEB STIFFENERS) USING S4 & B33	37
FIGURE 81 - MAXIMUM DEFLECTION EVOLUTION FOR THE 3 RD CASE STUDY (FREE WING + FLANGE & WEB STIFFENERS)	37

I. Introduction

The main goal of the simulation has been to investigate the Linear Static behaviour of the front of a vehicle structure by using ABAQUS Finite Element package. This report must clearly explain the modelling approach, how the models have been created and the reasons of the choices. After reading this report, people must be convinced that the model results can be trusted and use them to either carry on in the product design process or improve the structure by reviewing shapes and materials.

First of all, the report gives an overview of the case studies by outlining the main elements of the structure and the environment. Then, the geometry, meshing, convergence results and post-processing steps have been detailed for each case study and model used. By way of conclusion, a brief summary has been written in order to remind the important assumptions, remarks and results obtained.

II. Overview of the problem

1. What is the objective?

Concretely, the objective of this CAE simulation is to compute different discretised physical models to understand how the car structure reacts considering the physical restraints and the suspension loads taking in account the weight of the vehicle. Including all these parameters in the finite element models the post-processing steps lead to displacements and stresses values, which help to analyse the results and approve or not the simulation. Models must guarantee thanks to the post-processing results, i.e. stresses and deformations, that the physical properties of the structure remain in the elastic state, otherwise the simulation does not have any sense in this case. The general assumption of the Linear Elasticity state is small-deformation (small displacements/rotations and strain <1%).

Finite Element Analysis requires several different models to allow engineers to criticize the solutions so as to make sure that the simulation can be trust. Therefore various models have been designed using various kinds of structural elements with a view to offering multiple approaches by ensuring better results.

2. What is known?

A. Geometry

The front end of a vehicle structure is perfectly symmetric, thus the geometry used for the simulation can be limited to the front inner wing of a car (*see pictures below*).

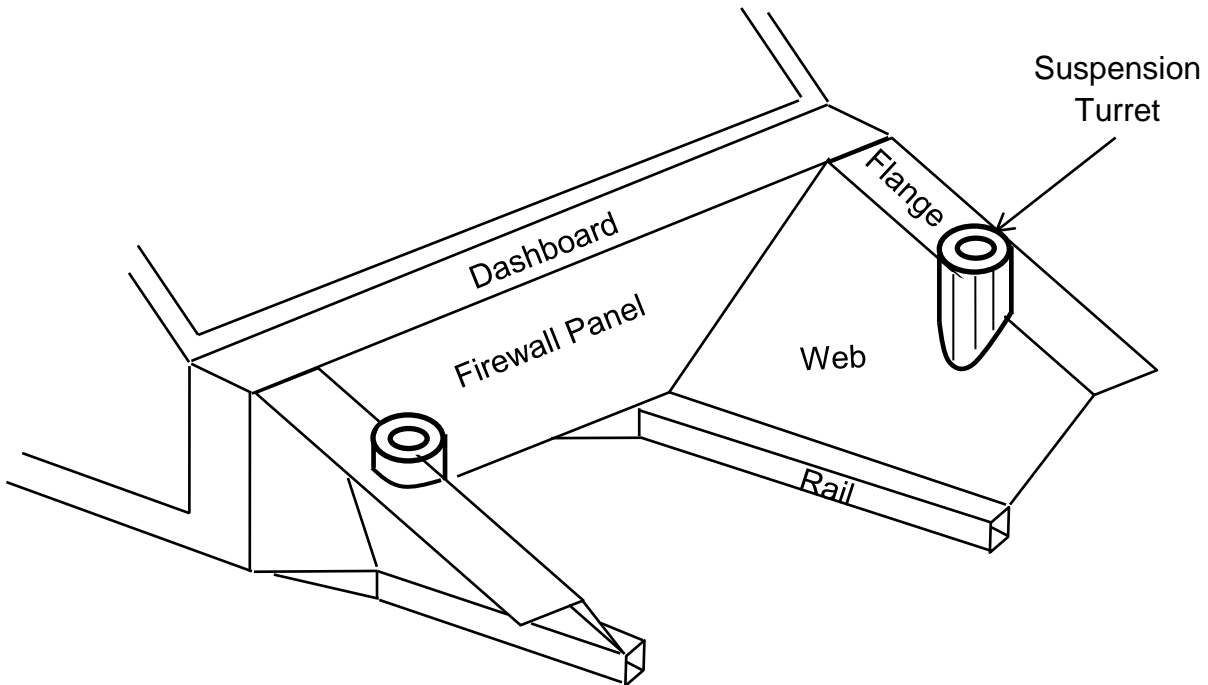


Figure 1 - Simplified representation of the Front Inner Wing assembly of a car

SYMMETRY

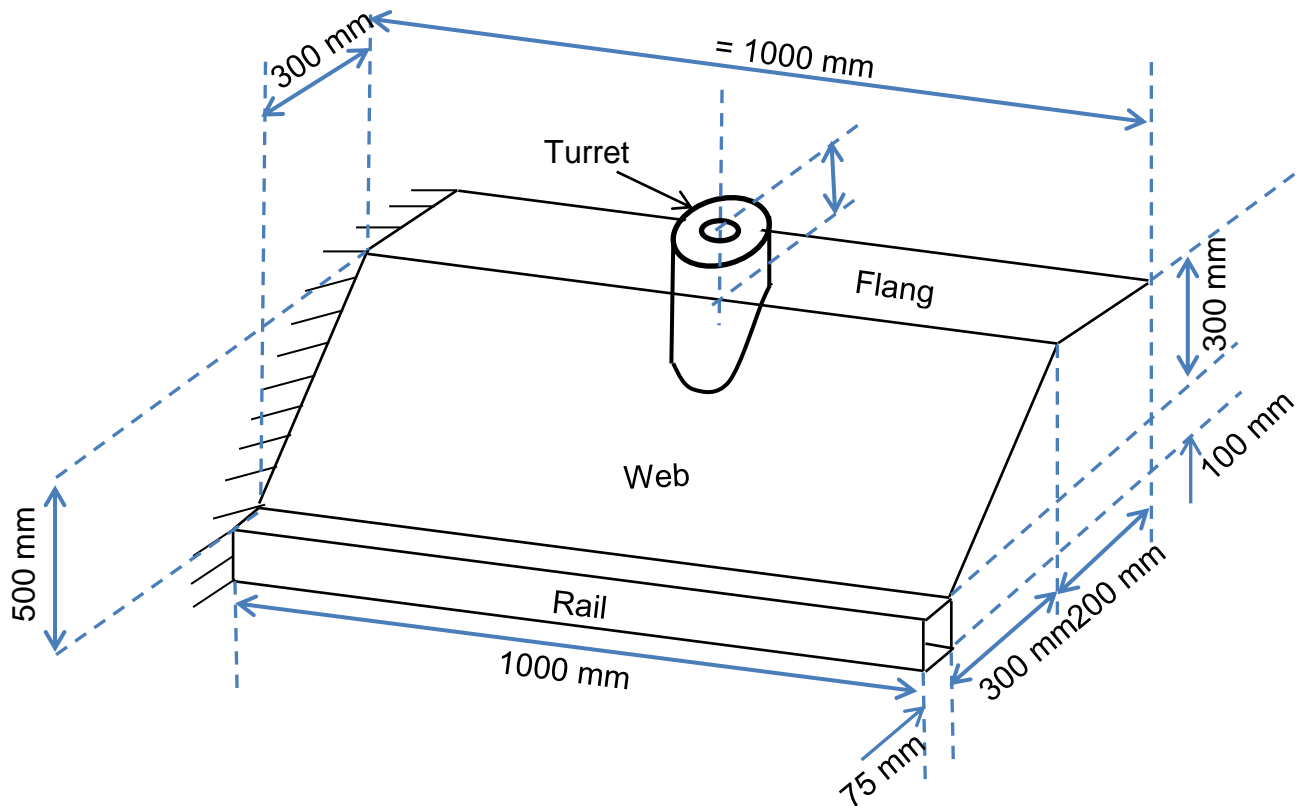


Figure 2 - 1st case study: Free wing

B. Material

The thickness and the material properties for each part of the wing are the following:

Part	Thickness (mm)	Material	Young's Modulus (MPa)	Poisson's Ratio
Turret	3.0	Steel	210 000	0.33
Flange	1.5	Aluminium	72 000	0.33
Web	1.0	Aluminium	72 000	0.33
Rail	2.5	Aluminium	72 000	0.33

It is important to notice that all these elements are made from uniform material.

C. Vehicle load

The vehicle has a total weight of 10 kN (1000 kg) distributed 60/40% between the front/rear. The analysis is for a 1g vertical symmetric load case and it can be assumed that the resultant force may be taken as acting vertically and is distributed over part of the suspension turret cap.

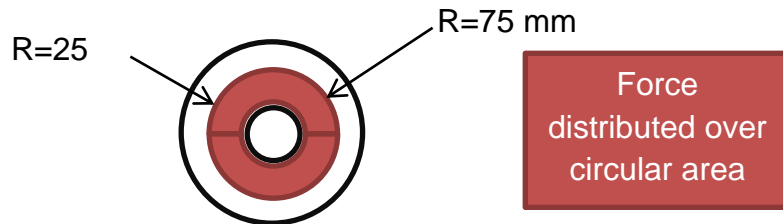


Figure 3 - Detail of Turret cap

3. Three case studies

A. Free wing

The first case study corresponds to the front wing (*cf. Figure 2*) without any stiffener. Nevertheless, the results show large displacements of the structure which means that the material properties do not remain in the elastic state. In this case two ways allow solving the problem, either the structure was designed to work in the plastic state, thus a Non Linear simulation must be undertake, or in another hand the geometry of the car body can be redesigned in order to make it stiffer. In this project the second choice has been selected using square stiffeners.

B. Free wing and outboard flange stiffener

The first reinforcing consists in adding only one 10x50 mm stiffener along the outer edge of the flange (*cf. Figure 4*) since it is the area where the displacement is maximal for the free wing case.

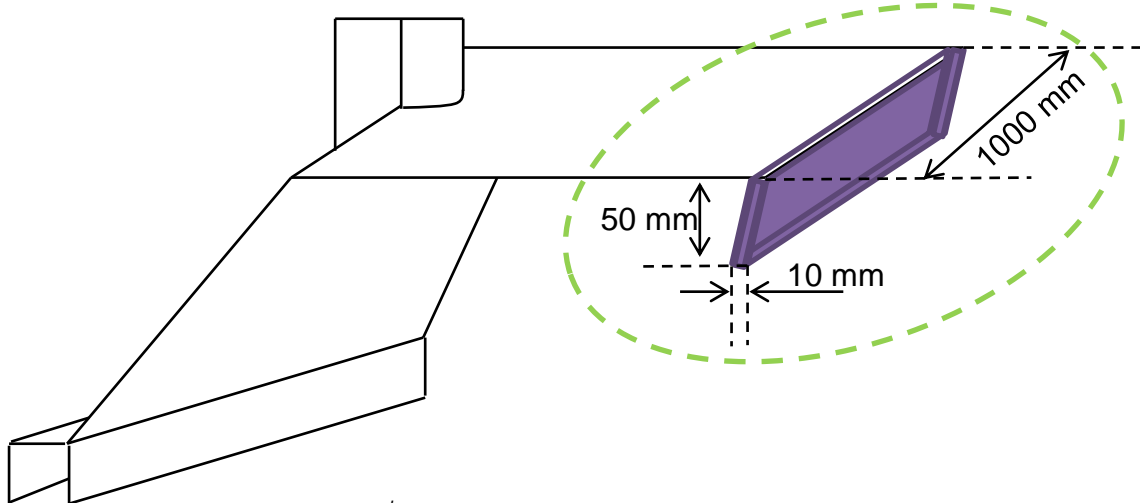


Figure 4 - 2nd case study: Free Wing + Flange stiffener

C. Free wing and stiffeners along the flange and web

Lastly, the last case study is the same than before adding two 10x10mm square stiffeners along the web.

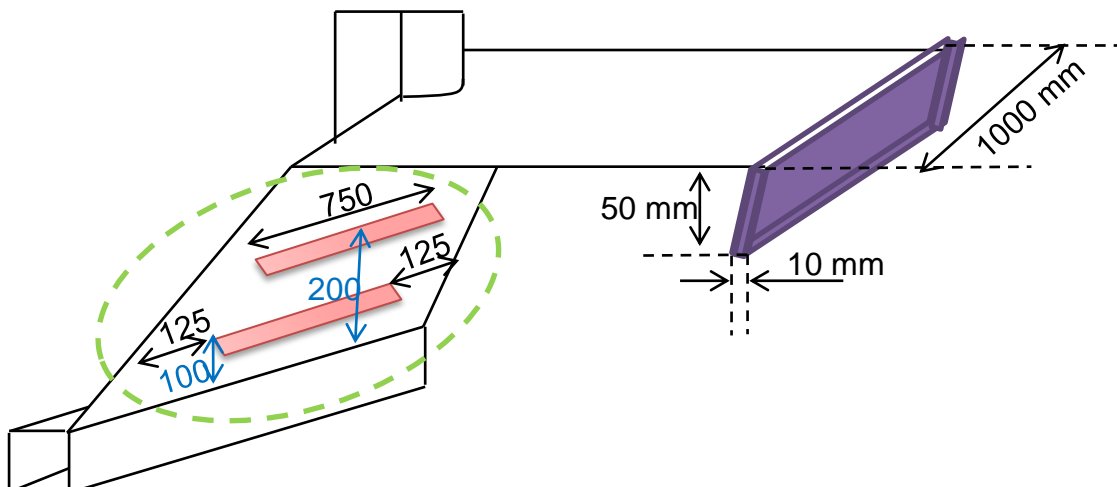


Figure 5 - 3rd case study: Free Wing + Flange & Web stiffeners

III. Calculations and assumptions

1. Rail assumptions

The design of the rail may cause trouble regarding the choice of the element: is it a beam or a shell? To answer to the question some calculations have been done to have a first idea before to start the simulation, even though it is sometimes difficult to make sure of the assumptions made.

⊕ Euler-Bernoulli beam:

- Definition: typical dimensions in the cross-section should be less than about 1/15 of typical axial distances (slenderness ratio) for transverse shear flexibility to be negligible.

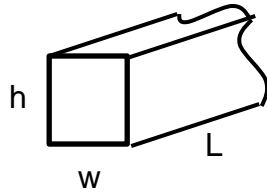


Figure 6 - Beam's properties

With: $L=1000 \text{ mm}$; $w = 75 \text{ mm}$ and $h=100 \text{ mm}$

- $L/15 = 1000/15 = 66.6 \text{ mm}$
- ⇒ w and h are > L/15, therefore the Euler-Bernoulli's hypothesis is not approved.

⊕ **Timoshenko beam:**

- **Definition:** typical dimensions in the cross-section should be less than about 1/15 of typical axial distances and up to 1/8.
- $L/8 = 125 \text{ mm}$
- ⇒ **L/15 < w and h < L/8, therefore the Timoshenko's hypothesis is approved.**

Timoshenko's hypothesis means that the beam is considered as thick beam, which carries transverse shear deformation, i.e. the cross-section does not remain perpendicular to the neutral axis, so the transverse shear stiffness values must be calculate.

- ⊕ **Shell:** Despite the Timoshenko's theory has been approved, the rail could be a big beam element, therefore a second geometry has been created allowing shell elements use in order to have a different point of view on the behaviour of the structure. Having a thickness smaller than 1/15 of the other lengths, the thin shell theory, Kirchoff's Theory, is satisfied (i.e. the shell normal remains orthogonal to the shell reference surface).

2. Web and Flange assumptions

At first sight, both the web and the flange have one dimension, the thickness, which is significantly smaller than the other dimensions. The load being along y axis, therefore they cannot be considered as membrane elements since they allow only in-plane forces. Consequently, the shell elements which carry membrane and bending forces have been preferred in this case.

3. Turret assumptions

Like for the web and the flange, the turret shows one dimension smaller than the others. As the cap has a loading orthogonal to the mid-surface, bending response must be considered using shell elements.

4. Load

The weight of the car being 10kN distributed 60/40% between the front/rear, therefore a force of 6kN is distributed over the area defined on each turret cap. However, the simulation is focused only on one wing, as a result a force (F) of 3kN has been used in the models. Considering the dimensions provided in the assignment, the pressure has been defined as following:

- Area (A) = $\pi.(R^2 - r^2) = \pi.(75^2 - 25^2) = 15707.96 \text{ mm}^2$
⇒ 3000 N → 15707.96 mm²
↳ Pressure = F/A = 3000/15707.96 = 0.191 N/mm².

IV. 1st case study: Free Wing

1. Scheme

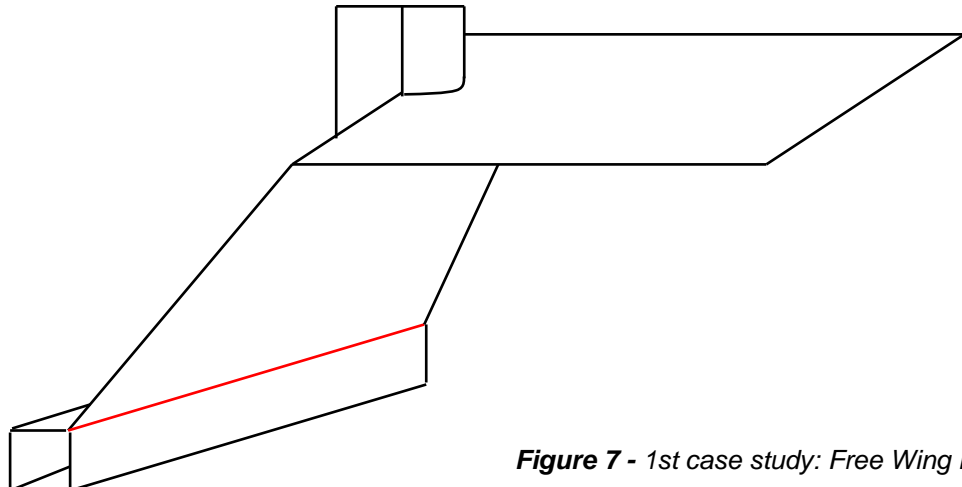
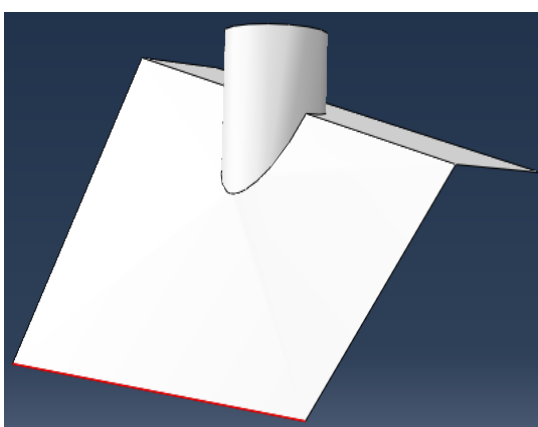


Figure 7 - 1st case study: Free Wing Model

2. Geometries

The structural design details are not tackled in this part but screenshots and explanations are provided ahead (cf. Appendix A).

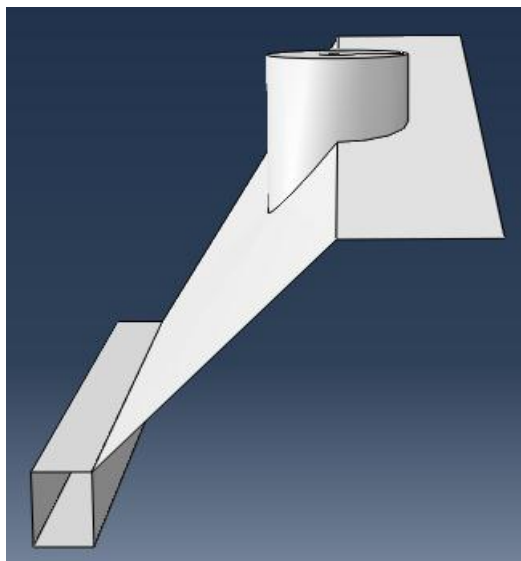
A. Shell & Beam elements Models



In the *rail assumptions*' paragraph it has been shown that the first range of models combines Timoshenko's beam and shell elements. In this case, the geometry of the rail does not need to be sketch since the cross-section is defined within the *arbitrary section* tool. Nevertheless, the edge common to the web and the rail (cf. Figure 8) must be defined as *stringer* in order to differentiate both parts.

Figure 8 - Geometry for Beam & Shell elements Models

B. Shell elements Models



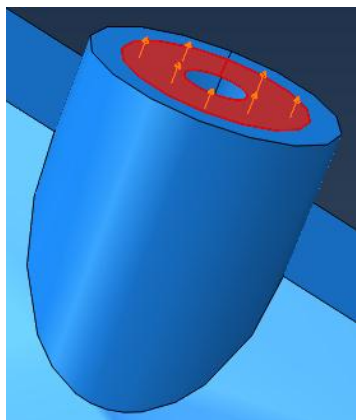
The second range of models has been used to study the behaviour of the single wing using shell elements for the discretisation. To mesh the rail with shell, it has been necessary to sketch its physical properties (height, width ...).

Figure 9 - Geometry for shell elements Model

3. Load & Boundary conditions

To set up the pressure load and the boundary conditions according to the different models a set and a surface have been defined. The advantage of defining in this way, means that the Boundary Conditions are applied to the Geometry, so if the structure is remeshed, it is not necessary to update the boundary conditions.

A. Load



Referring to the calculations made previously, a pressure equals to $0,191 \text{ N/mm}^2$ has been calculated to simulate the action of the suspension over the turret, however the turret cap must be split to define the circular area (*diam. 75mm*). The load remains the same for both geometries.

Figure 10 - Pressure Load 0.191 N/mm^2

B. Boundary conditions

The wing is directly attached to the rest of the vehicle structure, i.e. the flange is attached to the dashboard panel, the web is fixed to the transverse firewall panel and the rail is extended under the vehicle floor (cf. *Figure 1*). In other words, the concerned edge is fully fixed (encastred) that is why all the degrees of freedom have been constrained.

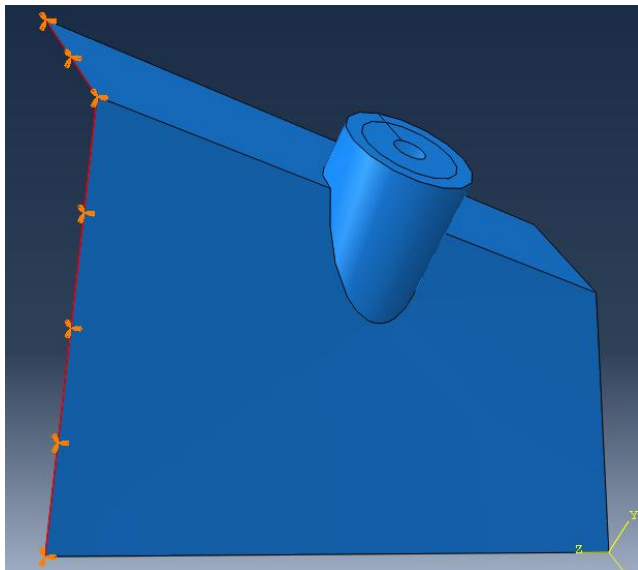


Figure 11 - BCs for Beam & Shell elements Models

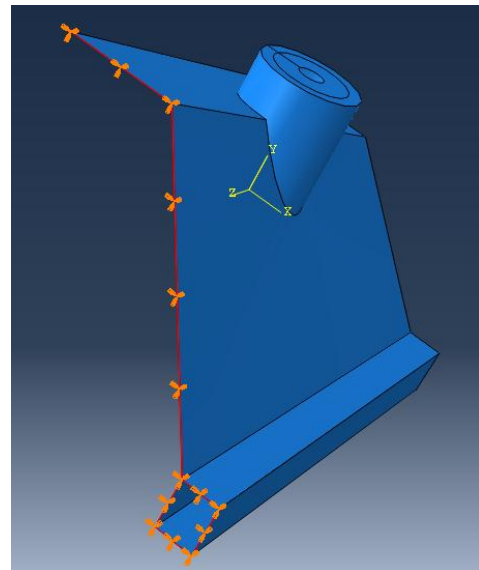


Figure 12 - BCs for Shell elements Models

4. Free Mesh

A free meshing method has been carried out in both geometries (*beam & shell elements and shell elements only*) to identify regions where further mesh refinement was needed.

A. Mesh & Elements formulation

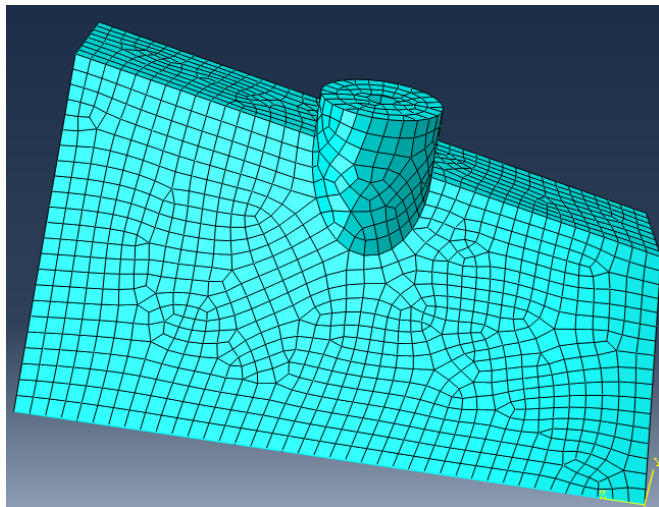


Figure 13 - Free Mesh using S4R & B31

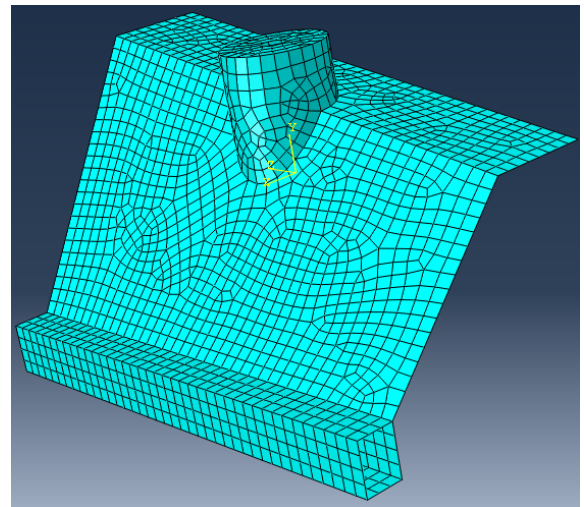


Figure 14 - Free Mesh using S4R

To ensure the continuity between each part, the geometry has been merged as dependent. At this stage, accuracy is not relevant (does not matter to have only quad elements); only an overview of the Von-Mises stress and displacements contours has an interest. Therefore a free mesh has been created using *Quad-Dominated* function to generate an acceptable quality mesh.

The element size has been calculated from the model using only shell elements (S4R). Since the rail is subject to bending, the vertical edge (100mm) must contain at

least two S4 elements or one S8 through the thickness to avoid nonsensical results for the stress. Therefore an element size of 25mm (100/4) has been chosen, thus there are four S4 elements through the thickness. Moreover, for modelling elements around hole, the minimum number of elements in critical region is twelve; this mesh has more elements than necessary using 25 mm element size.

Linear four-node general-purpose shell element with reduced integration (S4R) and Timoshenko's beam element using linear interpolation (B31) have been preferred to mesh the wing because both are computationally less expensive than any other element (e.g. S4 or B3).

B. Post-processing

a. Von-Mises Stress

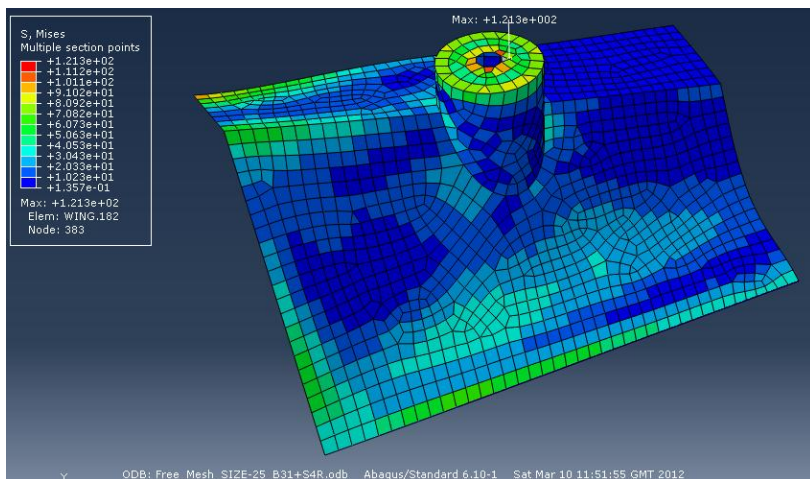


Figure 15 - Von-Mises stress for B31 & S4R

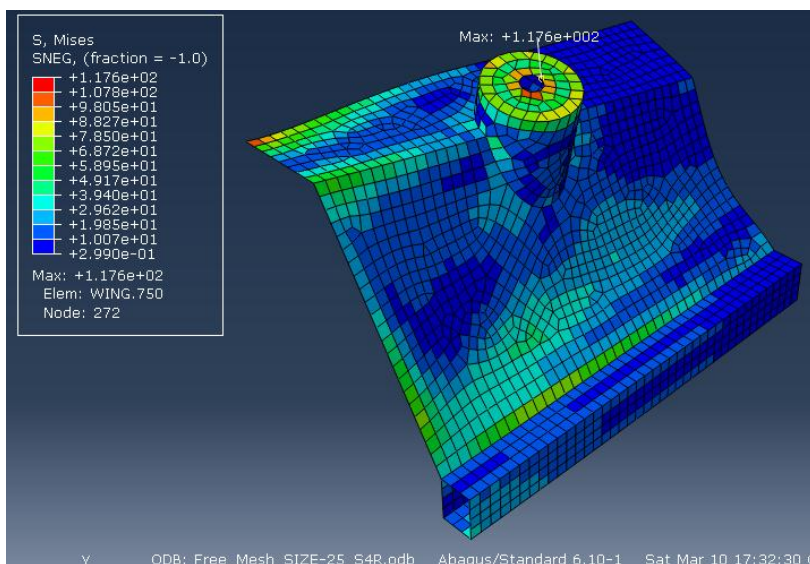


Figure 16 - Von-Mises stress for S4R

Observations:

- Both models seem to have roughly the same behaviour.
- The value of Von-Mises contours is high at each corner and along the fully fixed edge.
- The maximum of stress is located on the turret cap.
- The wing would be sized by the turret cap and the flange, i.e. since the highest amount of stress is in these parts, then they require more attention.

b. Deflection

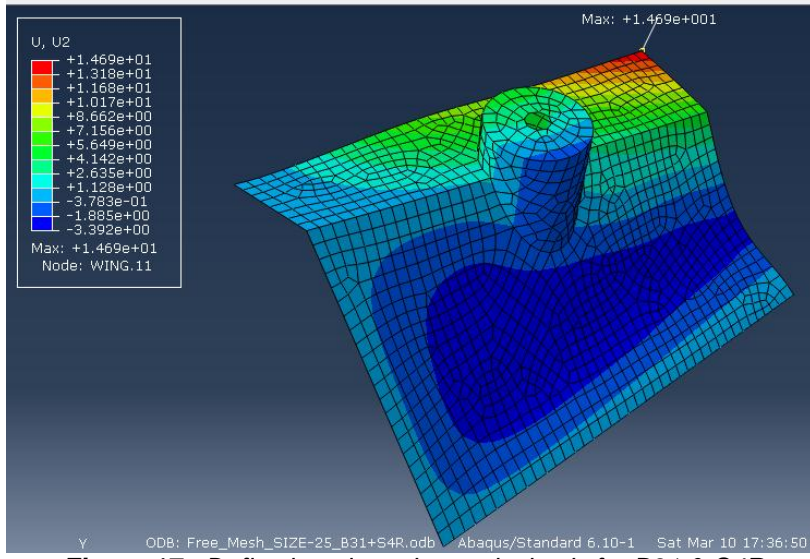


Figure 17 - Deflection along the vertical axis for B31 & S4R

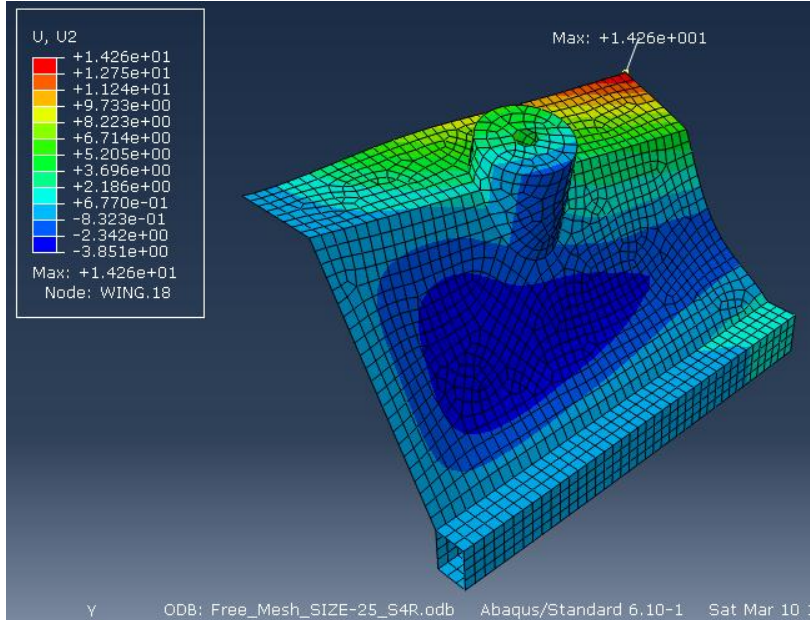


Figure 18 - Deflection along the vertical axis for S4R

5. Mesh

A. Partitioning of the structures

The more important things at the meshing step are the continuity of the mesh from one part to another and the controllability of its density. Both criteria have been ensured by merging all parts as an assembly Wing and by defining its grid as structured. Thus, any discretisation of the structure is propagated through –and–through. However, the body has been divided into smaller, piecewise surfaces with a view to getting uniform elements. During the partitioning stage, one rule must be respected: drawn out each partition to a boundary in order to have better transitions between two surfaces.

Observations:

- The maximum deflection is reached along the free edge, at the corner of the flange.
- The deflection of the right hand side of the wing seems to be more important than the left side.
- The structure moves upwards

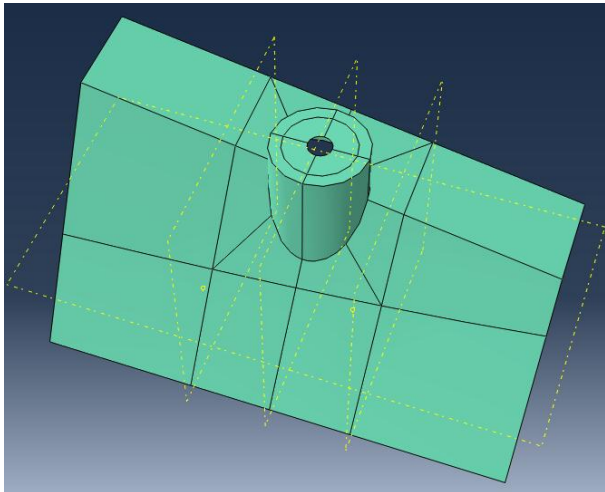


Figure 19 - Free Wing with partitions (beam & shell Models)

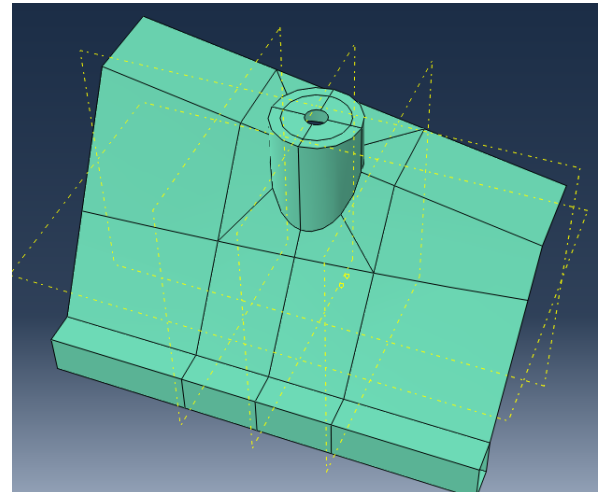


Figure 20 - Free Wing with partitions (shell Models)

B. Convergence

In finite element modeling, a finer mesh typically results in a more accurate solution. However, as a mesh is made finer, the computation time increases. A convergence study has been performed, thus a grid which is satisfactorily balance between accuracy and computational cost has been chosen.

Thanks to the free mesh models it has been proved that the rail is not relevant in the analysis since the Von-Mises stress and the deflection along the vertical direction are not really high. That is to say that it does not affect the convergence of the models, therefore the mesh convergence has been performed with only one geometry that represent the models combining beam and shell elements. To show that the model converges several element sizes have been used: 50, 40, 30 and 20 mm.

The first model that converges is reached when both the maximum Von-Mises stress and the maximum displacement values do not change of $+/- 5\%$.

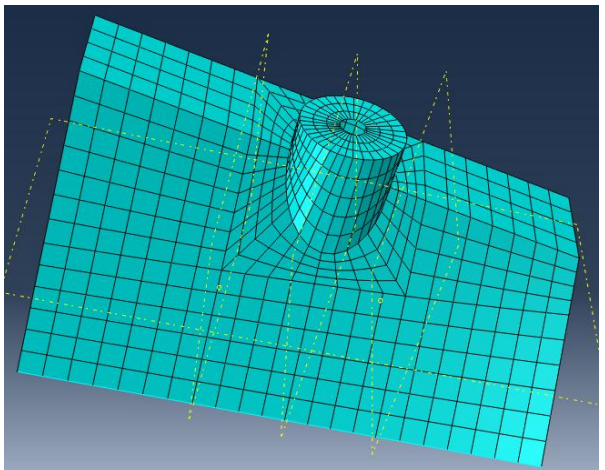


Figure 21 - Free Wing, SIZE 50, using B31 & S4R

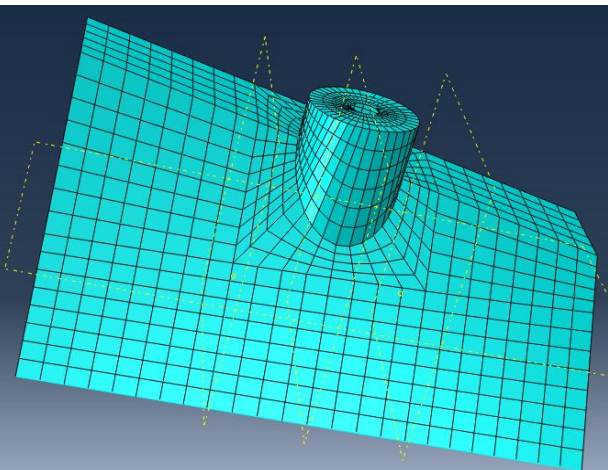


Figure 22 - Free Wing, SIZE 40, using B31 & S4R

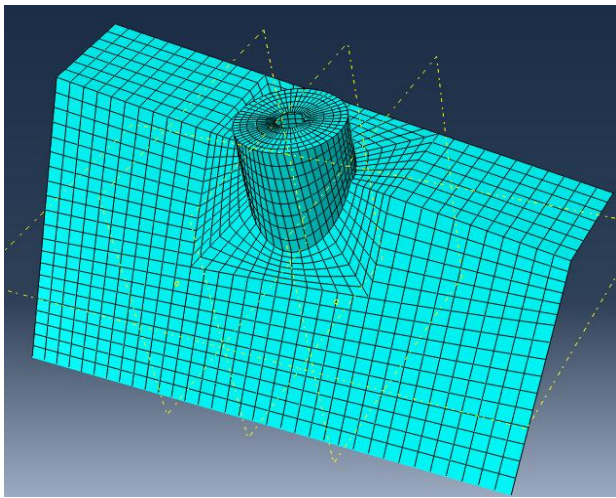


Figure 23 - Free Wing, SIZE 30, using B31 & S4R

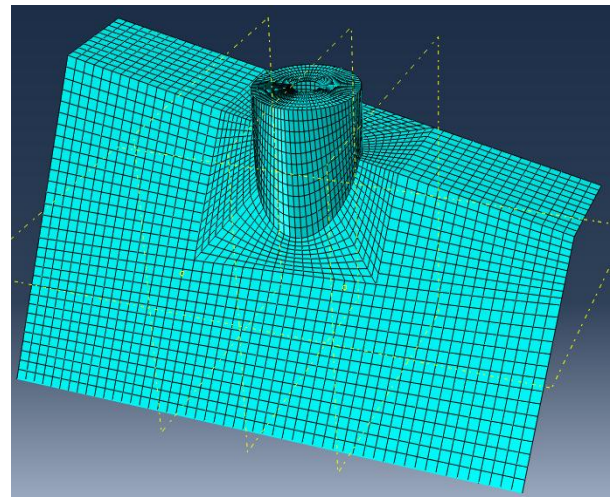


Figure 24 - Free Wing, SIZE 20, using B31 & S4R

The results of the maximum of Von-Mises stress and deflection obtained are thus:

MESH CONVERGENCE				
	Mesh 1: Element size 50	Mesh 2: Element size 40	Mesh 3: Element size 30	Mesh 4: Element size 20
MAX Von-Mises Stress (MPa)	90,17	96,48	97,9	103,3
State		NO CONVERGENCE	CONVERGENCE	
Max deflection (mm)	14,77	14,8	14,78	14,79
State		CONVERGENCE		
Von Mises Convergence	<i>Stress convergence reached for MESH 3</i>			
Displacement Convergence	<i>Deflection convergence reached for MESH 2</i>			

- ✚ $97.9 < 96.48 \times 1.05 \rightarrow$ The values of the MAX VM stress converge for an element size equals to 30.
- ✚ $14.8 < 14.77 \times 1.05 \rightarrow$ The values of the MAX deflection converge for an element size equals to 40.

The model seems to have a good response since the stress convergence is slower than the displacements convergence which is true in most cases.

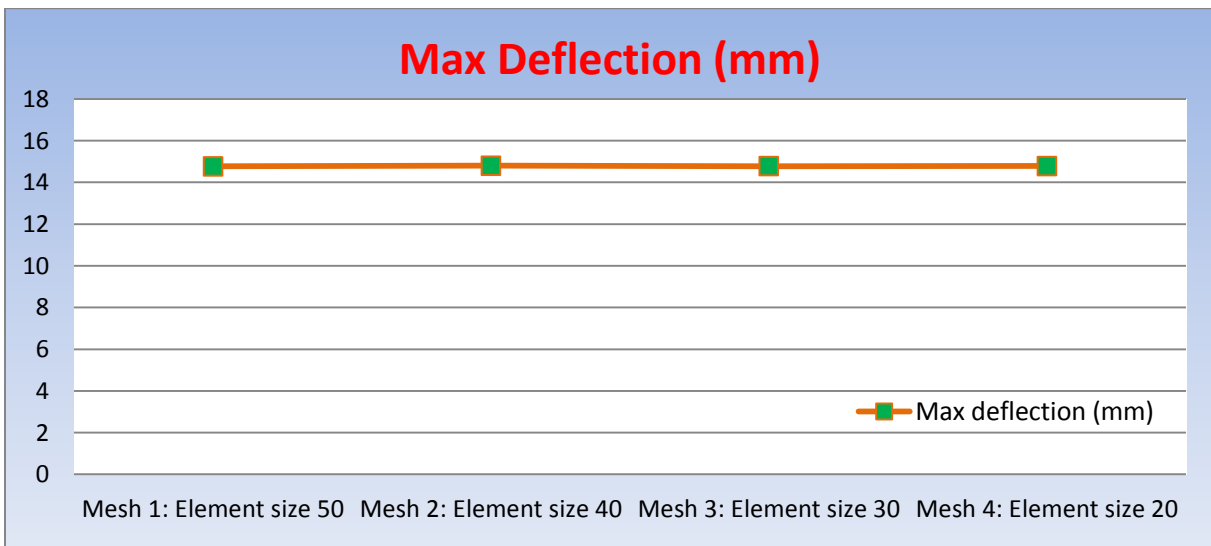


Figure 25 - Convergence of the maximum deflection

According to the previous graph, the displacement converges rapidly to 15 mm, the fact that displacement study requires coarser mesh is demonstrated here.

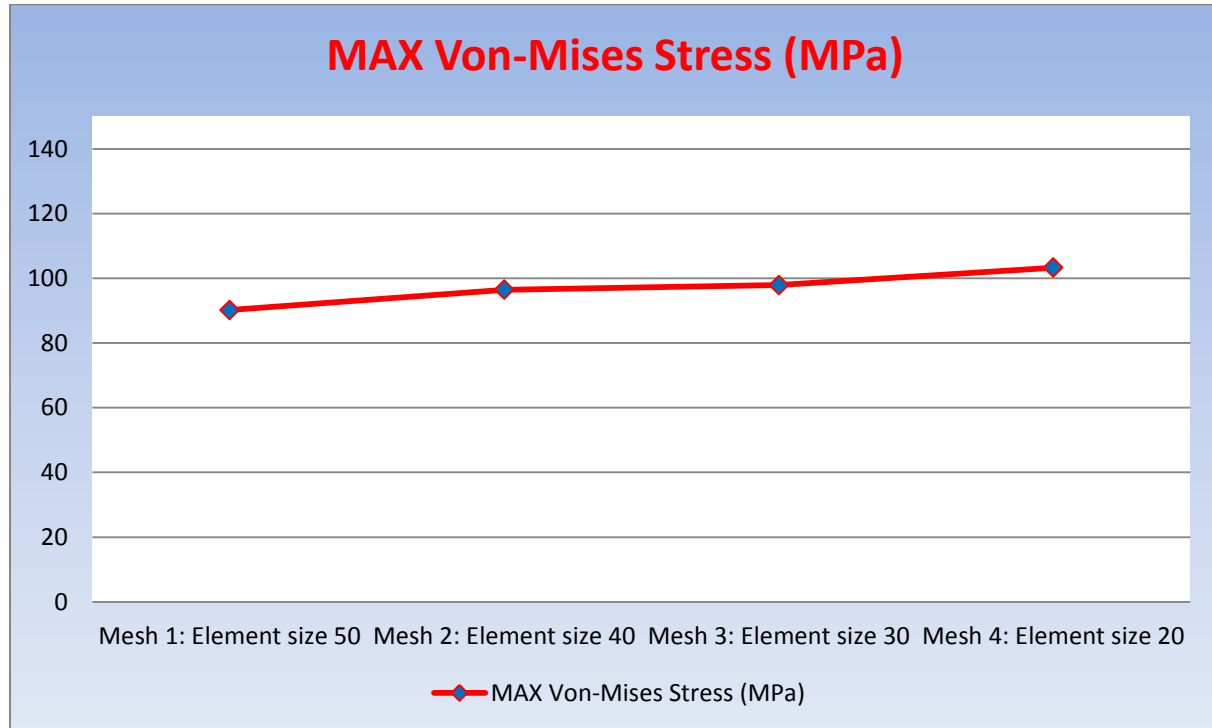


Figure 26 - Convergence of the Von-Mises stress

In other hands, the maximum Von-Mises stress converges to 100 MPa.

In conclusion, the best trade-off between accuracy and computing cost is the mesh 3 which use an element size equal to 30mm. That is why this mesh has been used to simulate all models for the three case studies, the only changes from one model to another are the type of elements used.

6. Models – Elements formulation

In order to have different feelings of the Free Wing's behaviour, five models have been designed involving different types of element to discretise the geometry. According to the kind of element(s), then either the Beam & Shell geometry or only Shell was utilised.

MODELS FOR FIRST CASE STUDY: FREE WING					
	Model 1 (Beam+shells)	Model 2 (Beam+shells)	Model 3 (Beam+shells)	Model 4 (Shells)	Model 5 (Shells)
Rail	B31	B31	B32	S4R	S4
Web	SR4	S4	S8R	S4R	S4
Flange	SR4	S4	S8R	S4R	S4
Turret	SR4	S4	S8R	S4R	S4

The first model combines 2-node Timoshenko beam elements and 4-node shell elements with reduced integration, rather than the second model use full integration. The difference is that reduced integration uses a lower-order integration to form the element stiffness, thus computational time and storage requirements are optimized.

The cross-section of the rail is loaded in a plane that it was designed and must undergoes elastic deformation, i.e., problem prone in-plane bending. In-plane bending requires elements that are not sensitive to distortion, and which avoid parasite locking. In this case S4 should be more accurate than S4R, thus Model 1 should give a better solution for the rail than S4 element.

The model 3 is a quadratic version of the modes 1 and 2, which is a 3-node beam element. The use of 3-node beam elements requires 8-node quadratic stress/displacement shell elements (S8) to ensure a good continuity. However, to make the model a little bit computationally less expensive, the S8 element with reduced integration (S8R) has been preferred. It is interesting to use this model when the main interest is stress concentration, e.g. in the turret cap. In most cases, a quadratic version of the elements fits the edge of a structure closer than linear, hence greater results are obtained.

NOTA:

- B31: Timoshenko's beam, linear interpolation, 2 node beam element (1st order)
- B32: Timoshenko's beam, quadratic interpolation, 2 node beam element (1st order)
- S4R: Linear, 4 node, general purpose shell, REDUCED integration
- S4: Linear, 4 node, general purpose shell, FULL integration
- S8R: Quadratic, 8 node shell, REDUCED integration

7. Post-processing

A. Equilibrium

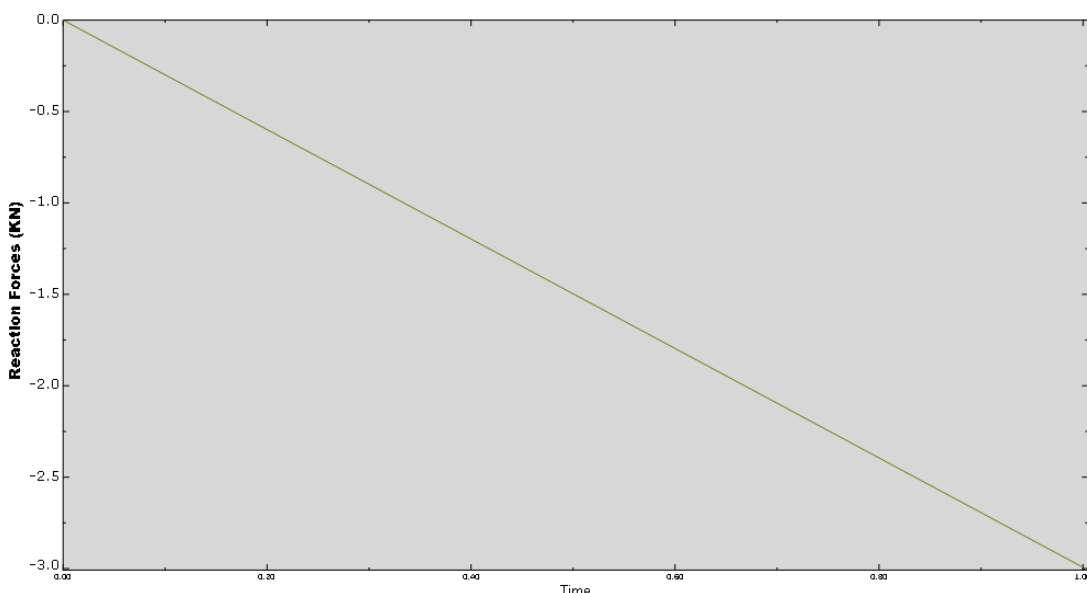


Figure 27 - Equilibrium study for the Free Wing

The equilibrium of the structure (Nodal Reaction Forces = Pressure Load applied) has been checked by plotting the nodal reaction forces in function to time step. The amount of Reaction Forces corresponds to the Pressure Load defined, 3000N (300Kg), thus the wing is in equilibrium.

B. Shell post-processing

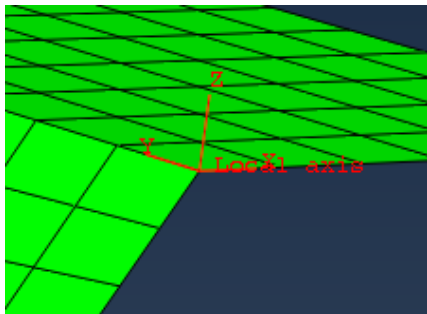


Figure 28 - Local set axis

In order to interpret the post processing properly, an additional local set axis (*cf. Figure 28*) has been created. The Z axis must remain orthogonal to the shell element, no matter what is the orientation of the section (*cf. Figure 29*).

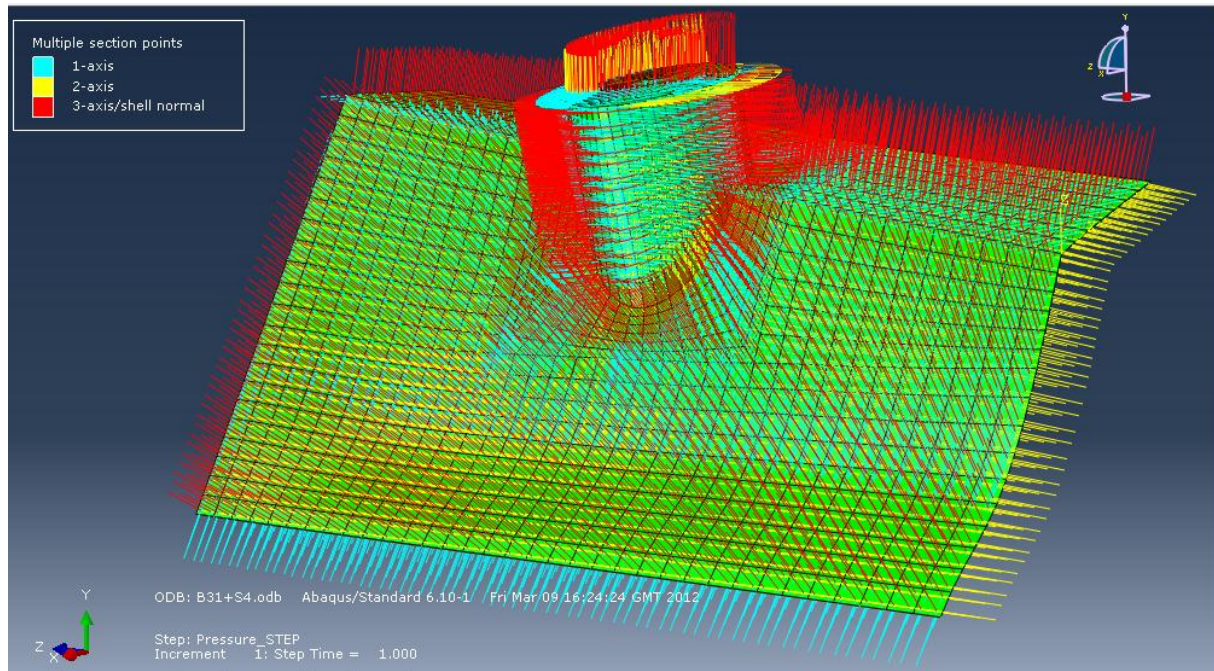
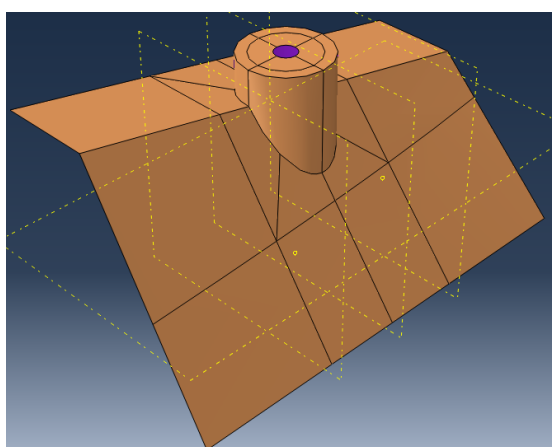


Figure 29 - Material directions



The brown faces correspond to the “top” surfaces in the positive normal direction and are called the SPOS face. The “bottom” surface, i.e. purple, is in the negative direction along the normal and is called the SNEG face.

Figure 30 - Shell definition

C. Stress post-processing

a. Von-Mises (VM) contours

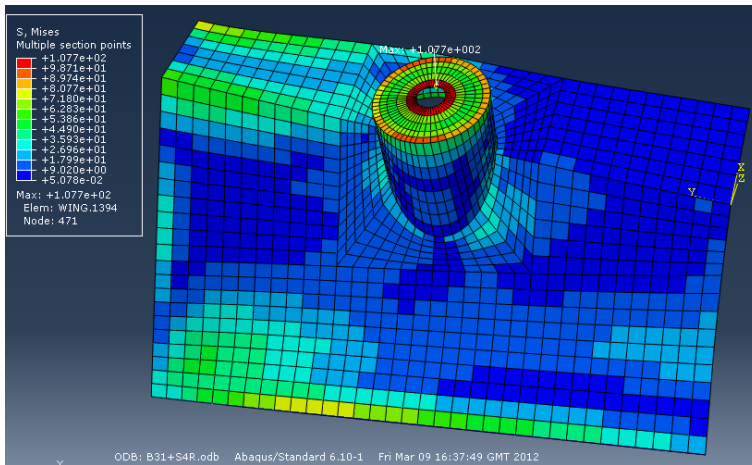


Figure 31 - VM stress for 1st case study (Free Wing) using B31 & S4R

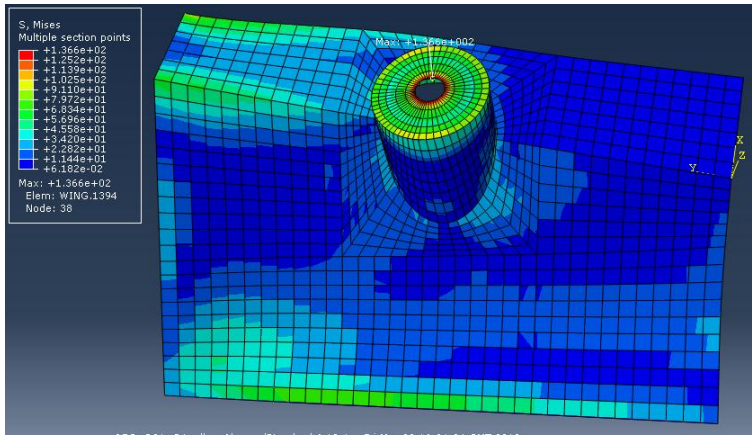


Figure 32 - VM stress for 1st case study (Free Wing) using B31 & S4

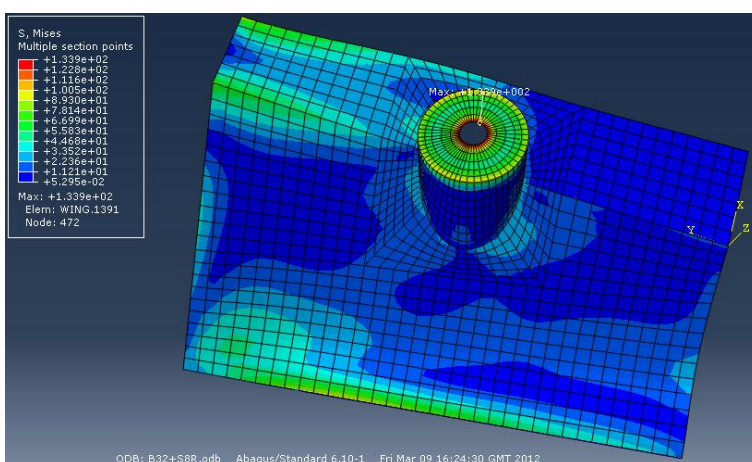


Figure 33 - VM stress for 1st case study (Free Wing) using B32 & S8R

Observations:

- The max Von-Mises stress value is equal to 136.7 MPa and converges to 124 MPa.
- The stress distribution is non-symmetric.
- There is a stress concentration at the edges of the turret cap.
- S8R elements are in general more accurate than others to capture high gradients of stress and ensure a good continuity in the contours.

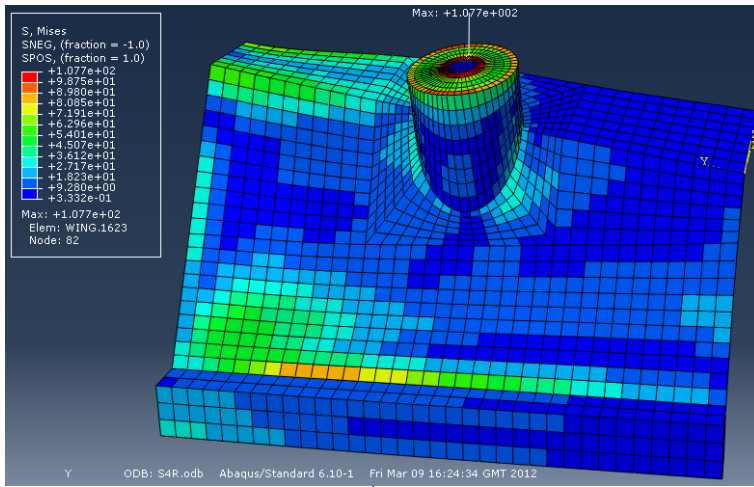


Figure 34 - VM stress for 1st case study (Free Wing) using S4R

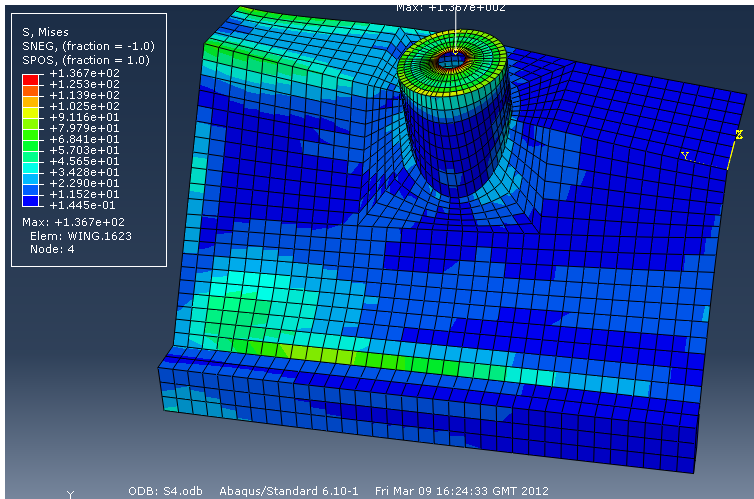


Figure 35 - VM stress for 1st case study (Free Wing) using S4

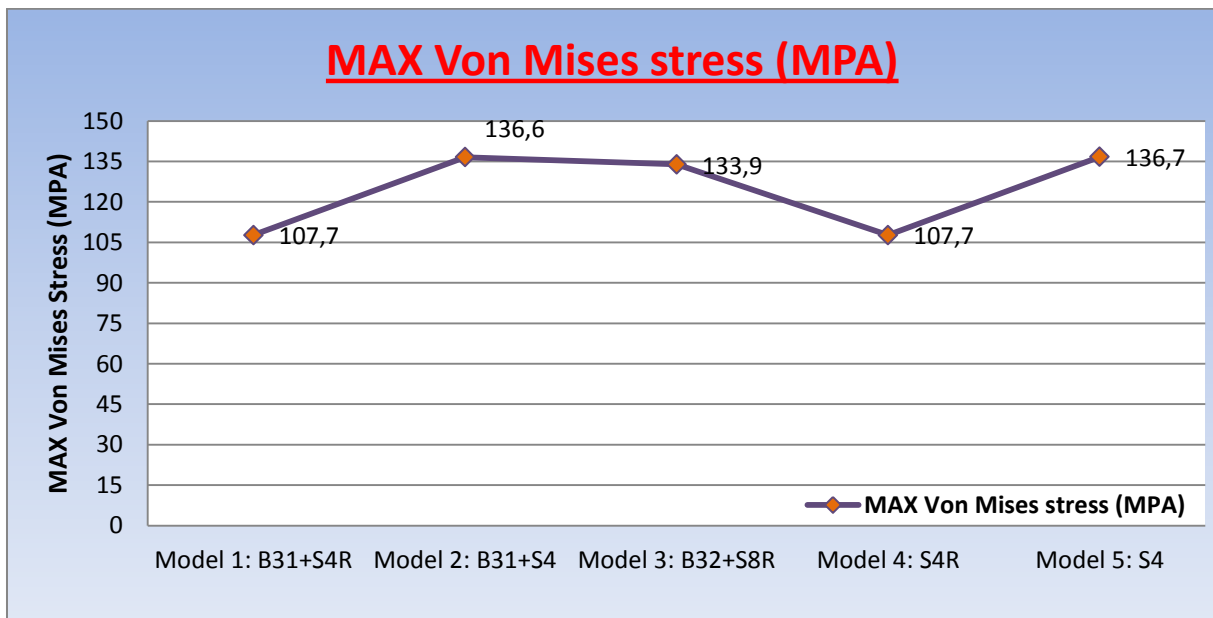


Figure 36 - Maximum Von-Mises stress evolution for the 1st case study (Free Wing)

b. Tension/Compression – SPOS/SNEG

If we look at S22 (stress in Y local axis), ABAQUS allow us to plot either the “top” stress contours or “bottom” stress contours of a shell element. All parts are subject to bending (tension/compression), thus this function is useful to make sure that the wing behaves properly, i.e. the tension/compression within “top”/“bottom” surfaces can be checked.

For example, in the Model 5 (S4 elements), we are able to make sure whether shell elements behave properly (tension in one side and compression in the other one) or not.

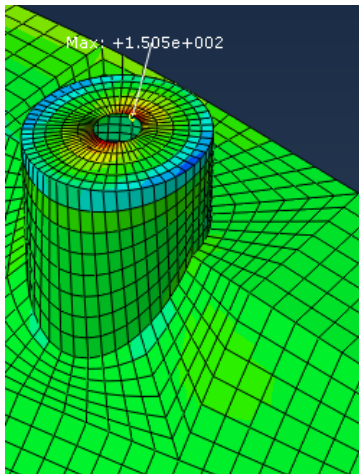


Figure 38 - Shell element behaviour

According to the figure 17 and shell's assumptions we should acknowledge opposite stress values in “top” and “bottom” surface which prove bending response. The easiest way to study bending is to focus on the turret cap since its deflections is obvious.

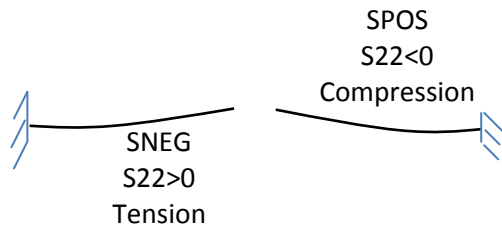


Figure 37 - Shell's behaviour expected for the shell elements

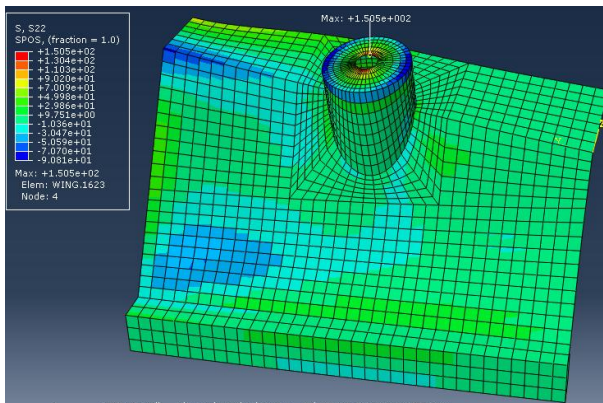


Figure 39 – SPOS S22 Stress for 1st case study (Free Wing) using S4

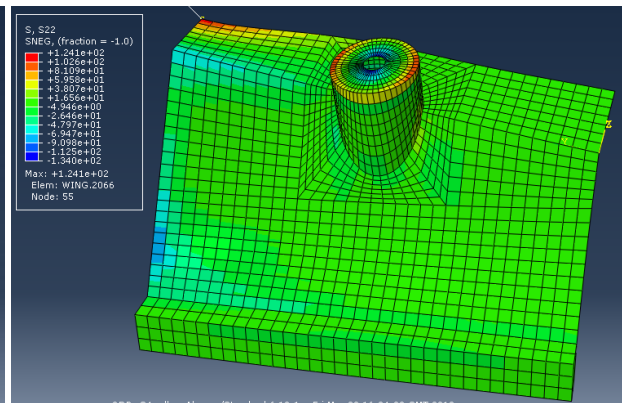


Figure 40 - SNEG S22 Stress for 1st case study (Free Wing) using S4

Having a look on the SPOS (cf. Figure 37), the S22 stress contours show negative values (between -70 and -90 MPa), then the “top” face is in compression as expected rather than the SNEG (cf. Figure 39) is in tension since S22 is positive (between 102.6 and 124.1 MPa) as expected as well.

D. Displacements post-processing

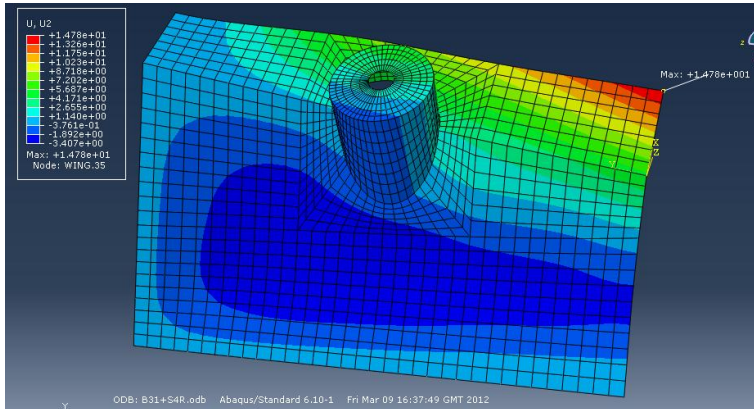


Figure 41 - Displacements for 1st case study (Free Wing) using B31 & S4R

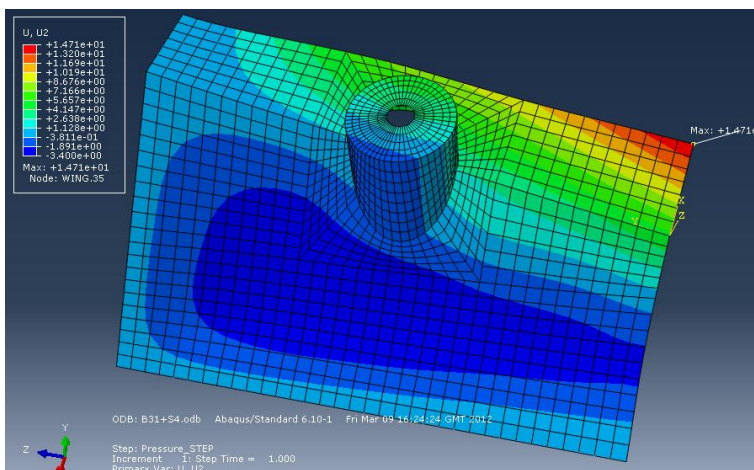


Figure 42 - Displacements for 1st case study (Free Wing) using B31 & S4

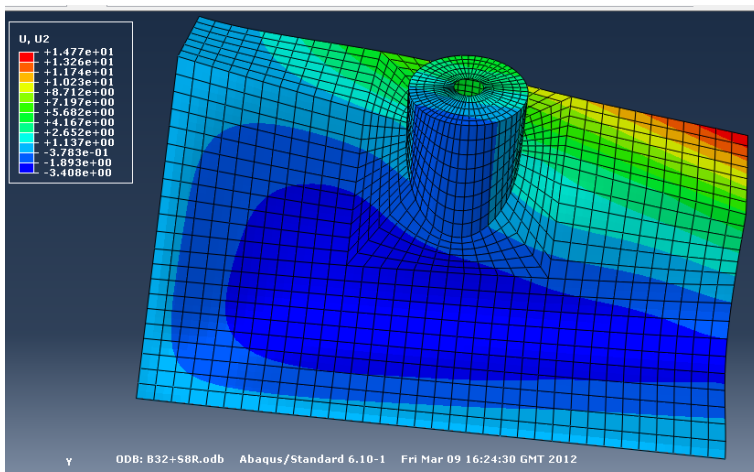


Figure 43 - Displacements for 1st case study (Free Wing) using B32 & S8R

Observations:

- The maximum deflection is equal to 14.78 mm and converges to 14.5 mm.
- The maximum deflection is obviously located at the free corner.
- The amount of displacement increases along the wing towards the free edge.
- The evolution of the displacements does not vary significantly which is normal since the mesh is pretty fine to evaluate deflection.

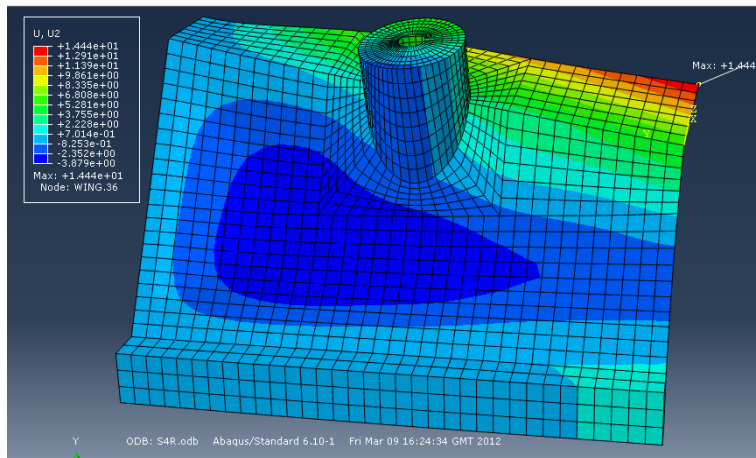


Figure 44 - Displacements for 1st case study (Free Wing) using S4R

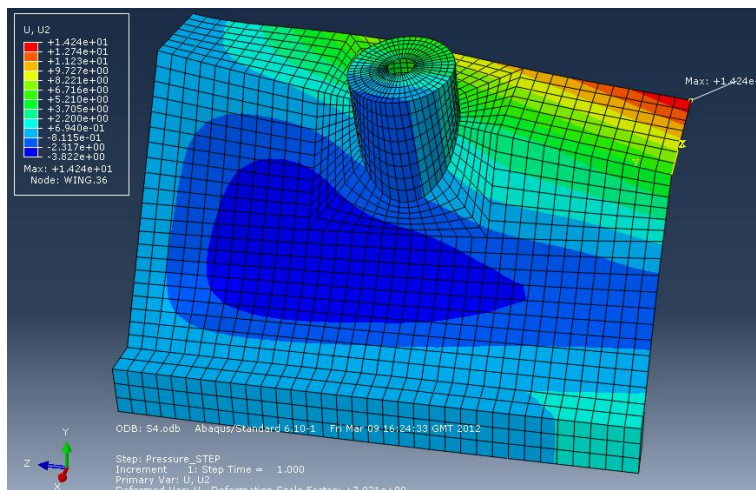


Figure 45 - Displacements for 1st case study (Free Wing) using S4

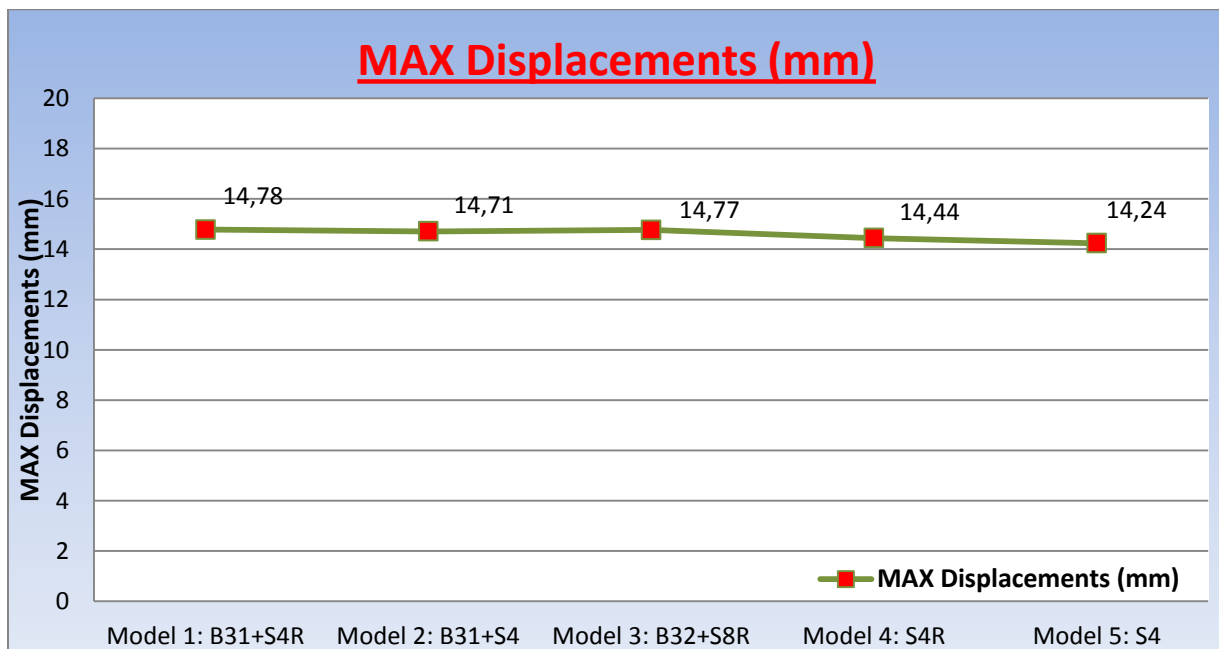


Figure 46 - Maximum Deflection evolution for the 1st case study (Free Wing)

It has been shown that stress values change according to the type of element chosen, which is normal and comforting. By improving the accuracy of the model, the maximum values of Von-Mises fortunately change and converge to a finite value of 135 MPa. Therefore, this analysis seems to be “believable” since the behaviour change according to the accuracy of the model and remains almost the same from one model to another.

Furthermore, use Von-Mises stress as yield criteria, allow us to know whether the material (steel and aluminium) remains in its elastic domain or not. The maximum Von-Mises value is in the flange and is equal to 136.7 MPa. The flange is made of aluminium and its elastic yield is equal to 240 MPa, so the material linearity is approved. However, the graph (*cf. Figure 45*) indicates 14.78 mm as maximum deflection, which is quite high. Hence the small-deformation assumption is not approved for this model. In this case, the model must be modified either by using a stronger material or improving the design of the part. Here the second choice has been preferred by adding one stiffener under the flange. This new design requires a new analysis.

V. 2nd case study: Free Wing + Flange stiffener

1. Geometry

The second case study corresponds to the reinforced Free Wing geometry (*cf. Figure 47*).

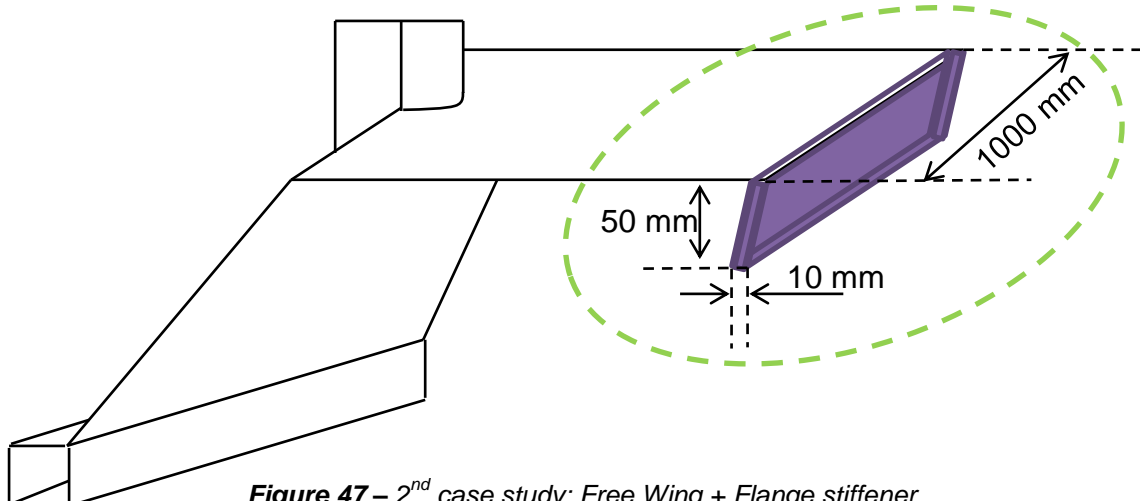


Figure 47 – 2nd case study: Free Wing + Flange stiffener

2. Load & Boundary conditions

The pressure load is the same as the beginning it is not necessary to modify it. The boundary conditions of the wing are also unchanged, i.e. one edge is fully fixed.

3. Mesh & Elements

The mesh used in the previous analysis (size 30 mm) has been kept here. Regarding the elements, their formulation is identical for this new modelling. Only the stiffener needs to be thought that is why a quick hand calculation has been done.

- 50×20 (height x 20) = 1000
- 10×10 (width x 20) = 100

The typical dimensions in the cross-section are less than about 1/20 of typical axial distances, thus transverse shear flexibility is negligible, and in other words Euler-Bernoulli's Theory (*plane section initially normal to the beam's axis remains plane and normal to the beam axis*) is approved. The simplest element to model an Euler-Bernoulli beam is B33 2-node beam element, which uses cubic interpolation functions.

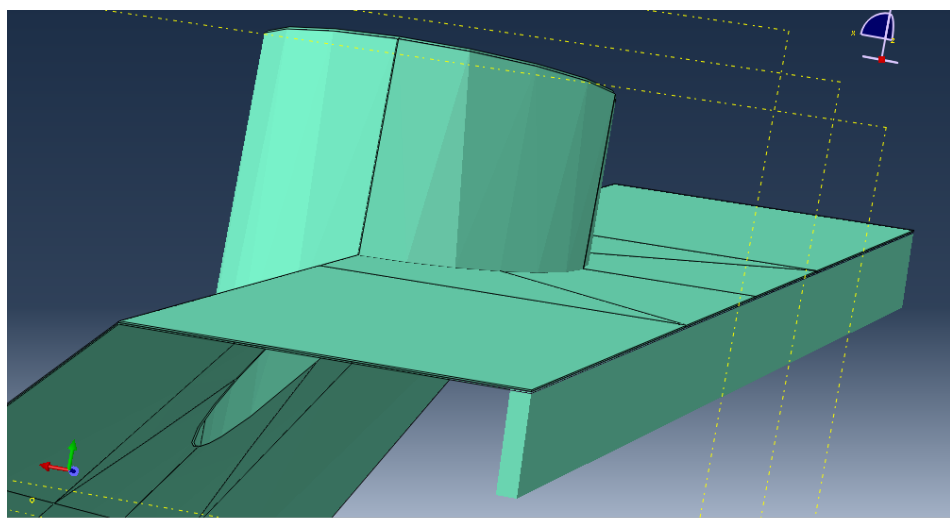


Figure 48 - Flange stiffener

4. Models

MODELS FOR SECOND CASE STUDY: FREE WING + FLANGE STIFFENER

	Model 1 (Beam+shells)	Model 2 (Beam+shells)	Model 3 (Beam+shells)	Model 4 (Shells)	Model 5 (Shells)
Rail	B31	B31	B32	S4R	S4
Web	SR4	S4	S8R	S4R	S4
Flange	SR4	S4	S8R	S4R	S4
Turret	SR4	S4	S8R	S4R	S4
Flange Stiffener	B33	B33	B32	B33	B33

All the models designed for the first case study have also been used to study the behaviour of the single wing rigidified by a stiffener. However, for the third model it is not possible to use a B33 element since S8R shell element requires 3-node beam, therefore B32 has been taken.

5. Post-processing

A. Equilibrium

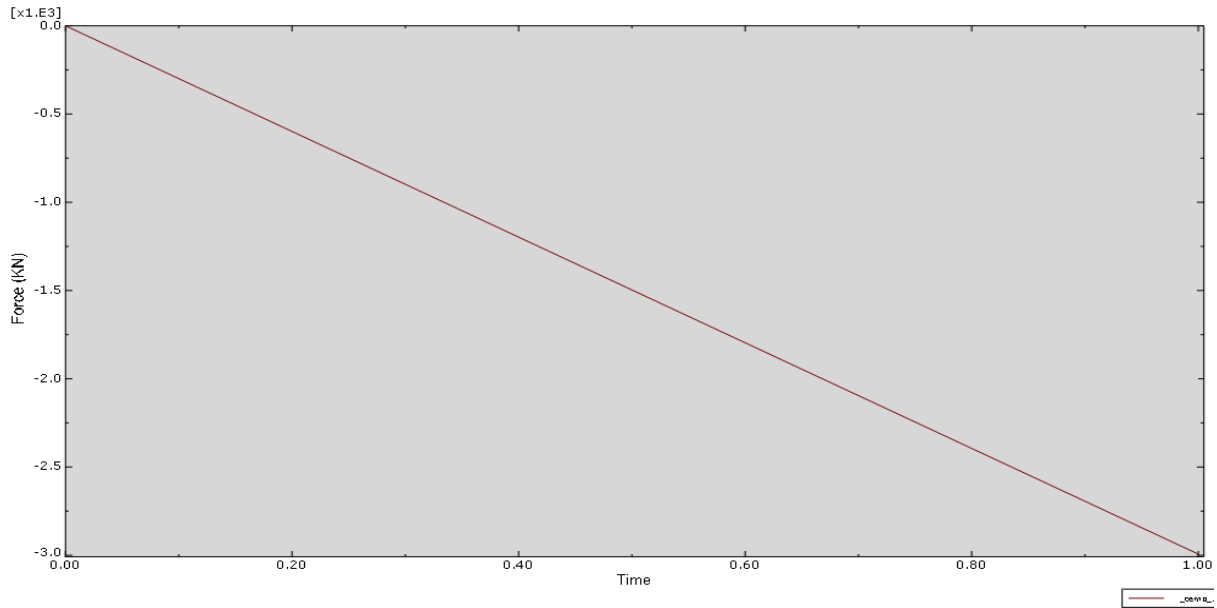


Figure 49 - Equilibrium study for the Free Wing + Flange stiffener

The equilibrium is checked since the sum of the reaction forces is equal to -3KN, i.e. a reaction of 3000N (300kg for 1g) downwards and it makes sense since the pressure is in the positive direction (upwards).

B. Shell post-processing

Still to check the coherence of the results, the bending response has been plotted. Thus the stress S22 contours enable engineers to make sure that the SNEG (bottom plane) of the shell elements are in tension ($S22>0$) and the SPOS (top plane) is in compression ($S22<0$).

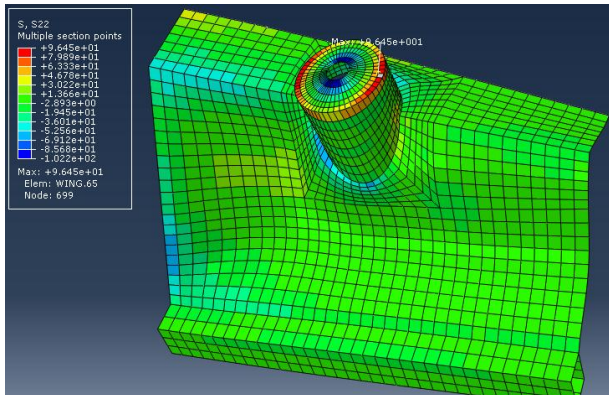


Figure 50 - SNEG S22 Stress for 2nd case study (Free Wing + Flange Stiffener) using S4 & B33

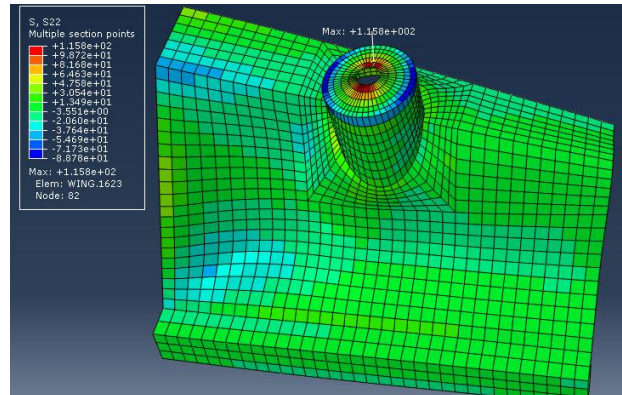


Figure 51 - SPOS S22 Stress for 2nd case study (Free Wing + Flange Stiffener) using S4 & B33

Both pictures above prove the good behaviour of the shell element.

C. Von-Mises stress contours

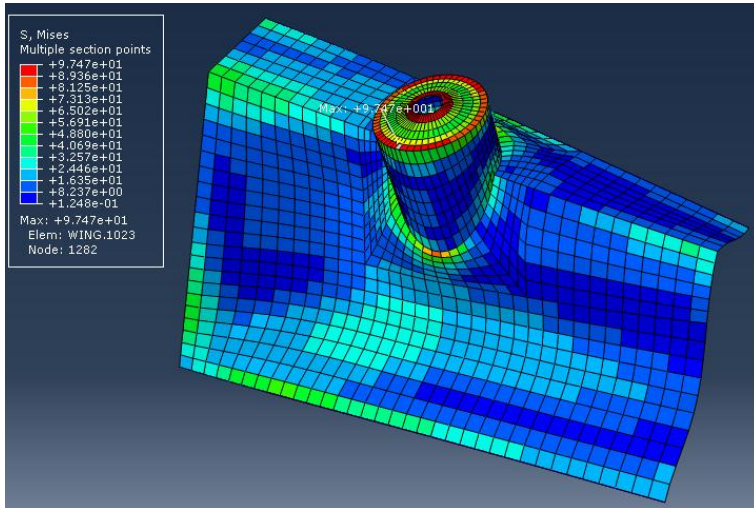


Figure 52 - VM stress for 2nd case study (Free Wing + Flange Stiffener) using B31 & S4R & B33

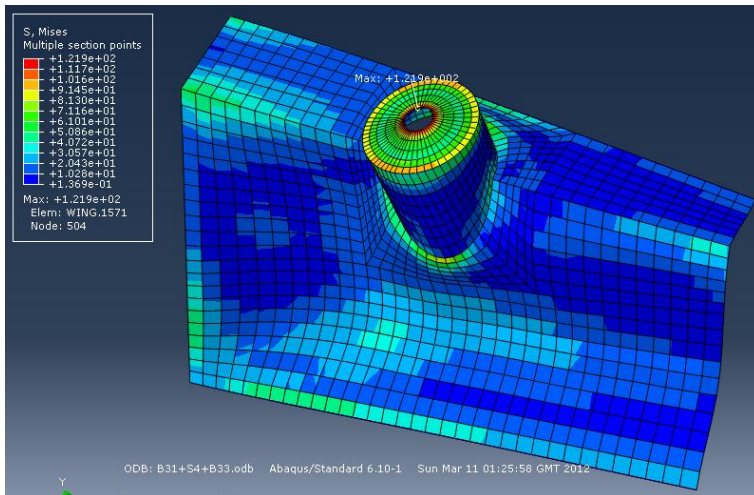


Figure 53 – VM stress for 2nd case study (Free Wing + Flange Stiffener) using B31 & S4 & B33

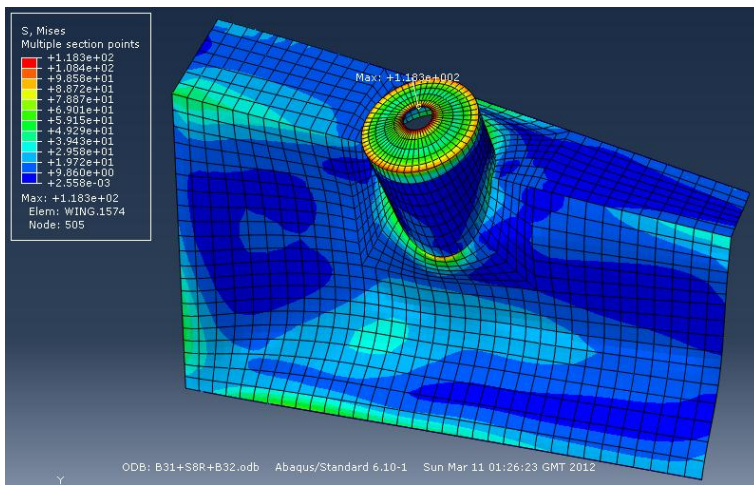


Figure 54 – VM stress for 2nd case study (Free Wing + Flange Stiffener) using B32 & S8R & B33

Observations:

- The maximum value of the Von-Mises criteria is 121.9 MPa and converges to 111 MPa.
- The structure is stiffer than the first geometry, then the maximum Von-Mises stress value decreases for each model.
- Comparing with the previous model it has been noticed that the Von-Mises stress contours are less important. The maximum is still located on the turret which is logical since the pressure force is applied over it.

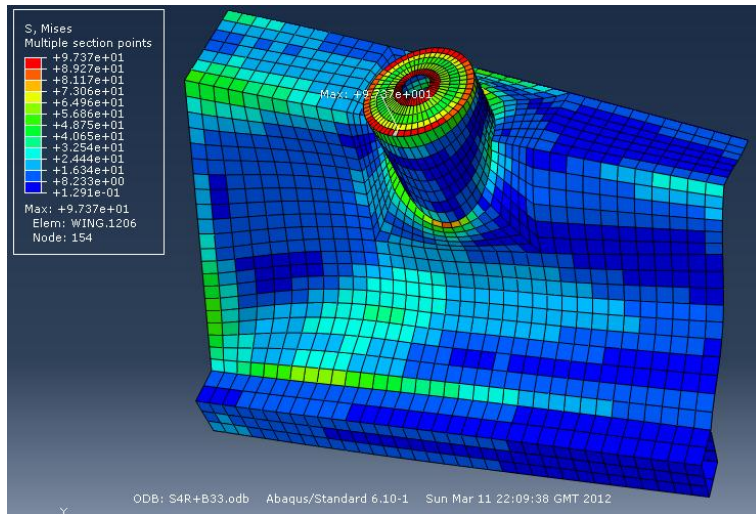


Figure 55 – VM stress for 2nd case study (Free Wing + Flange Stiffener) using S4R & B33

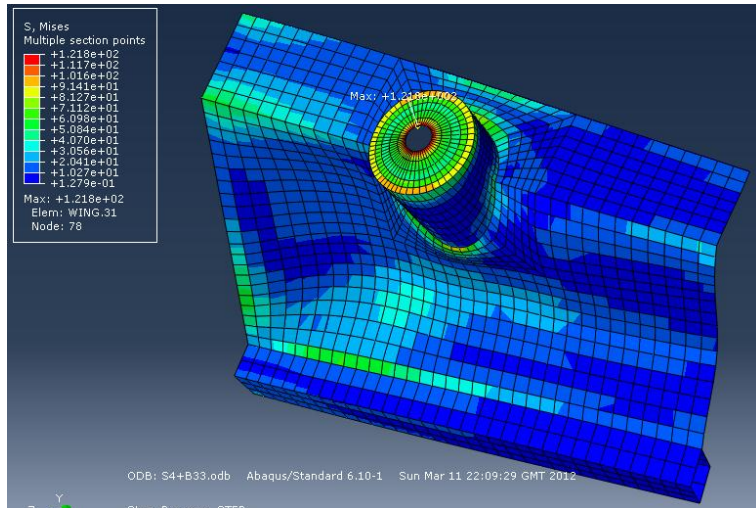


Figure 56 – VM stress for 2nd case study (Free Wing + Flange Stiffener) using S4 & B33

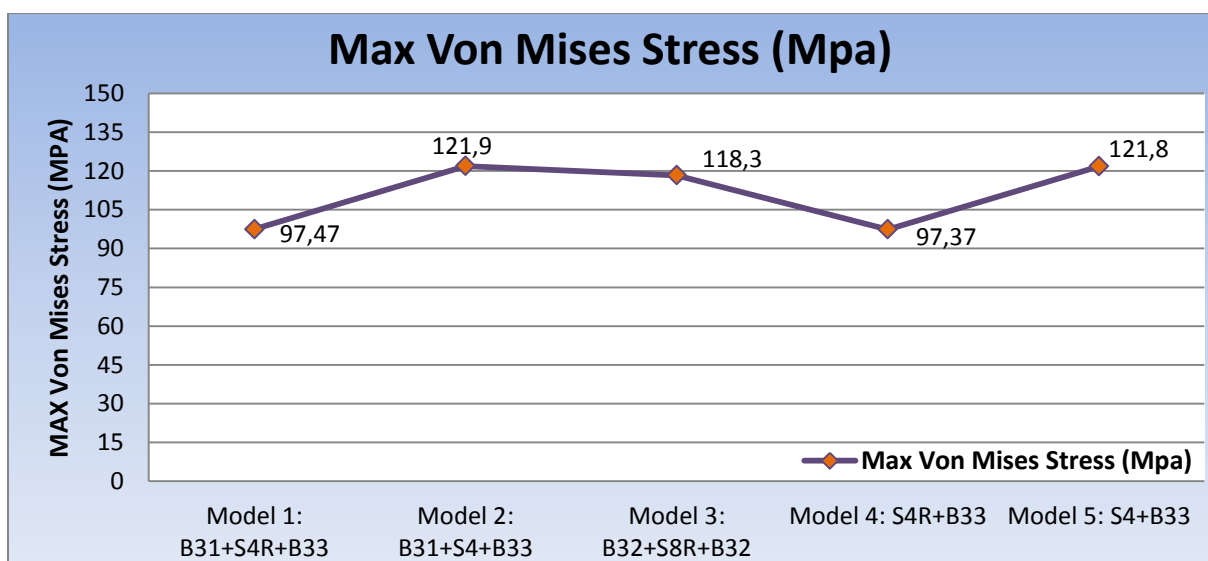


Figure 57 – Maximum Von-Mises stress evolution for the 2nd case study (Free Wing + Flange stiffener)

D. Displacements contours

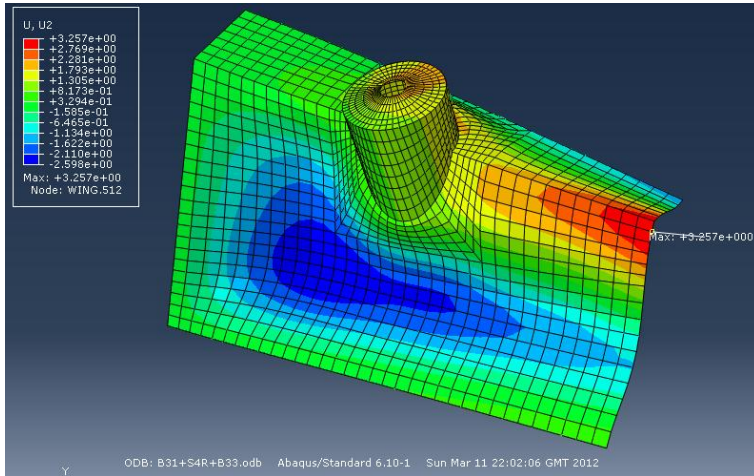


Figure 58 – Displacements for 2nd case study (Free Wing + Flange Stiffener) using B31 & S4R & B33

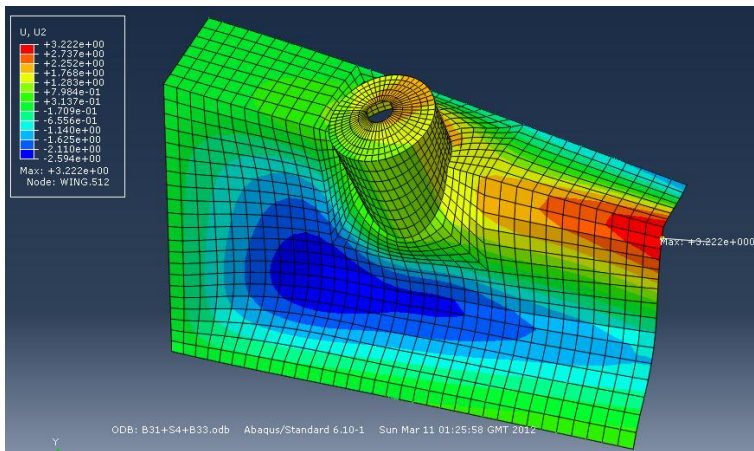


Figure 59 – Displacements for 2nd case study (Free Wing + Flange Stiffener) using B31 & S4 & B33

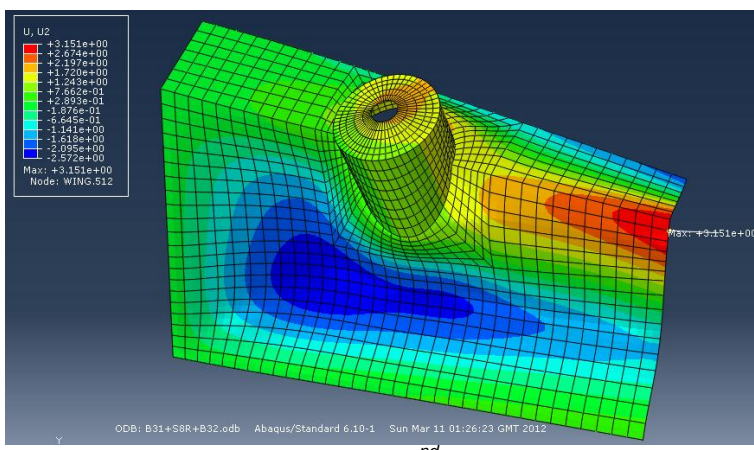


Figure 60 – Displacements for 2nd case study (Free Wing + Flange Stiffener) using B32 & S8R & B33

Observations:

- The maximum deflection 3.257 mm and converges to 3.2 mm. Nevertheless, in this case study the maximum displacement is at the junction of the web and the flange on the free side which seems logical as the corner of the flange is supported by the stiffener.
- The structure is stiffer than the first geometry, then the maximum Von-Mises stress value decreases for each model.

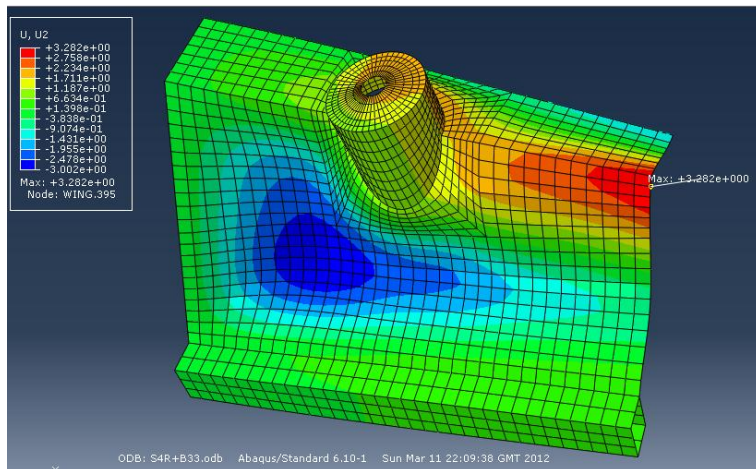


Figure 61 – Displacements for 2nd case study (Free Wing + Flange Stiffener using S4R & B33)

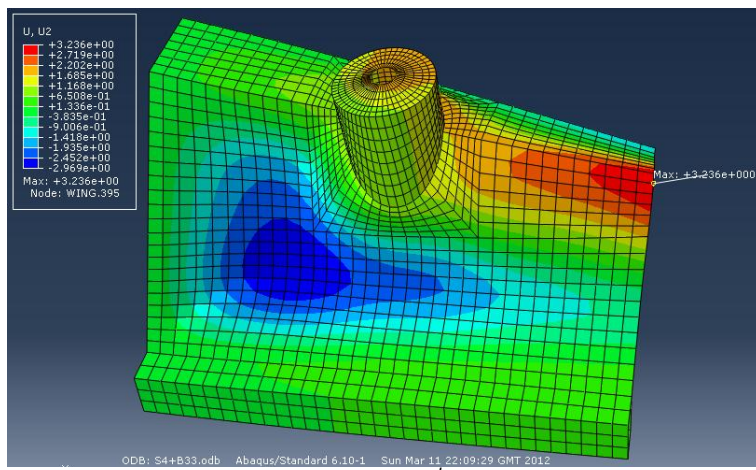


Figure 62 – Displacements for 2nd case study (Free Wing + Flange Stiffener) using S4 & B33

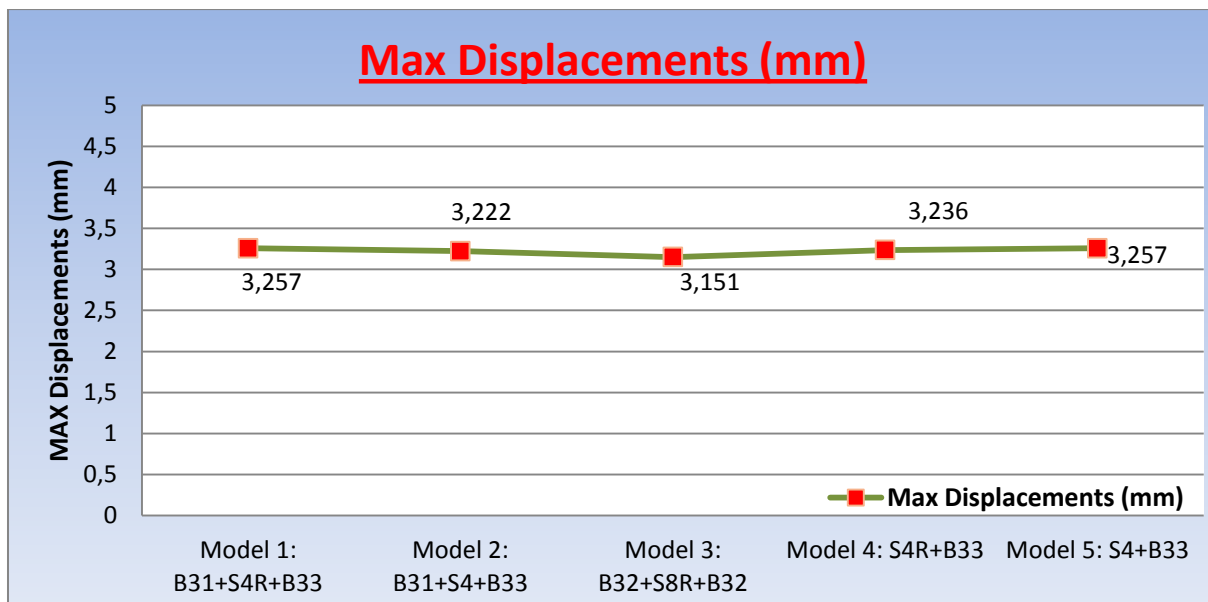


Figure 63 – Maximum Deflection evolution for the 2nd case study (Free Wing + Flange stiffener)

The use of a stiffener under the flange has a little bit improved the amount of stress in the structure, however it has considerably reduced the displacements and especially in the flange part. The maximum Von-Mises stress and deflection are respectively equal to 121.9 MPa and 3.257 mm, thus the structure does not exceed the elastic yield of the material.

VI. 3rd case study: Free Wing + Flange & Web stiffeners

1. Geometry

For the third model it has been decided to reinforce the web part by adding two 10x10x750mm stiffeners as well as the flange stiffener added at the previous case study (cf .Figure 63).

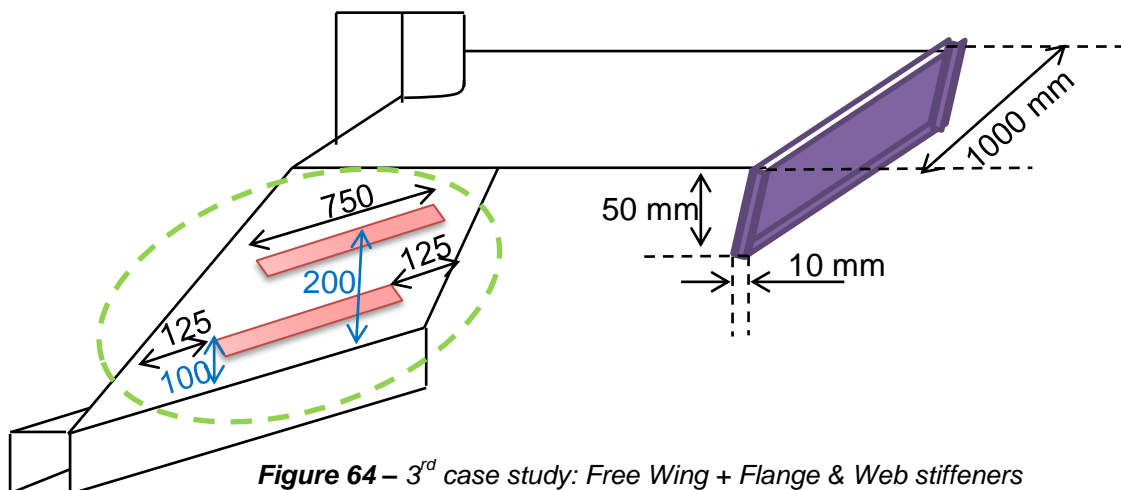


Figure 64 – 3rd case study: Free Wing + Flange & Web stiffeners

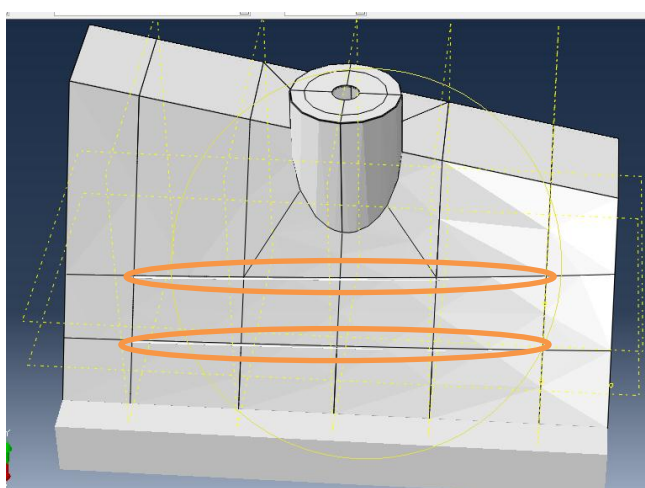


Figure 65 - New partitions for the 2nd case study

In order to add the stiffeners on the web it has been necessary to modify the partitions. Four planes (100/200 mm up to the rail part and 125mm from each side) have been designed in order to enable the creation of two stringers.

2. Load & Boundary conditions

The pressure load and the boundary conditions are unchanged, only the fully fixed set has been updated to take an account all partitions of the web.

3. Mesh & Elements

The mesh size equals to 30 mm has been conserved for this case, however the part has been remeshed because new partitions have been required to model beam elements (web stiffeners). All elements have been renewed, and Euler-Bernoulli's beam has been chosen for the web stiffeners.

- 10×20 (height x 20) = 200 mm <<< 750 mm, Euler-Bernoulli's theory is true.

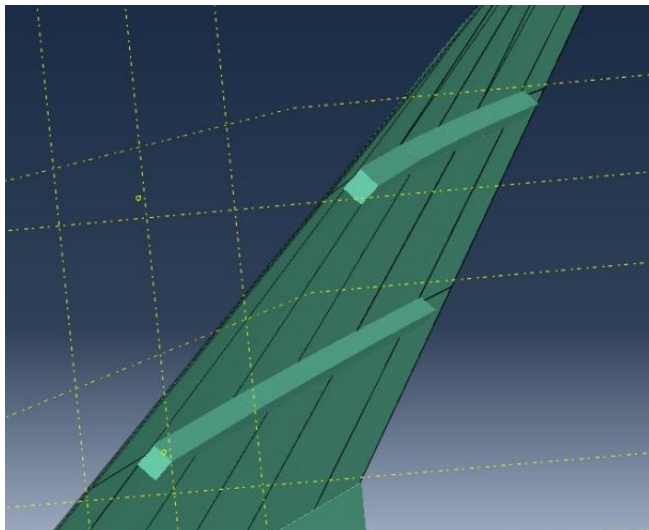


Figure 66 - Web stiffeners

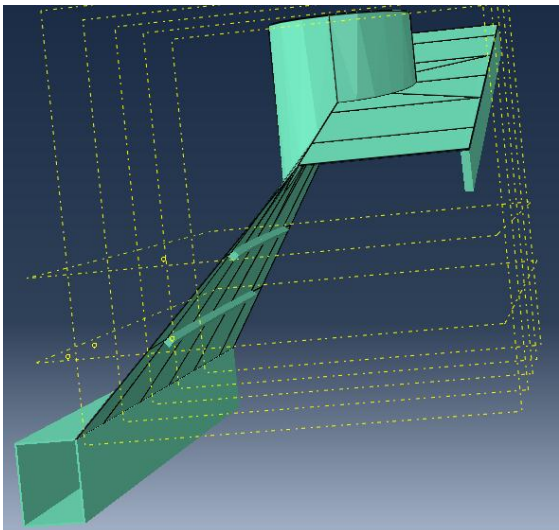


Figure 67 - Final part

4. Models

MODELS FOR THIRD CASE STUDY: **FREE WING + FLANGE STIFFENER + WEB STIFFENERS**

	Model 1 (Beam+shells)	Model 2 (Beam+shells)	Model 3 (Beam+shells)	Model 4 (Shells)	Model 5 (Shells)
Rail	B31	B31	B32	S4R	S4
Web	SR4	S4	S8R	S4R	S4
Flange	SR4	S4	S8R	S4R	S4
Turret	SR4	S4	S8R	S4R	S4
Flange Stiffener	B33	B33	B33	B33	B33
Web Stiffeners	B33	B33	B32	B33	B33

Models are the same as the second case study by adding B33 elements for the web stiffeners. As before it is not possible to use 2-node beam elements (B33) with eight-node shell elements (S8R), thus B32 has been chosen.

5. Post-processing

A. Stress post-processing

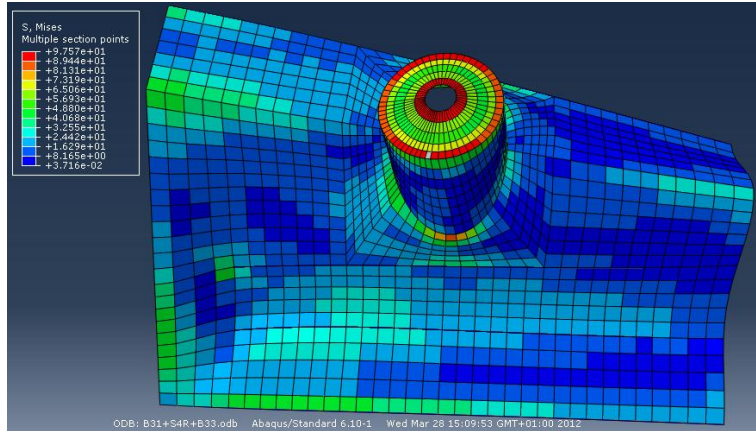


Figure 68 - VM stress for 3rd case study (Free Wing + Flange & Web Stiffeners) using B31 & S4R & B33

Observations:

- The maximum value of the Von-Mises criteria is 121.9 MPa and converges to 111 MPa.
- The maxima are the same as the Free Wing + Flange stiffener model and it is normal since they are always located at the turret cap. Hence both stiffeners on the web do not impact the amount of stress in general.

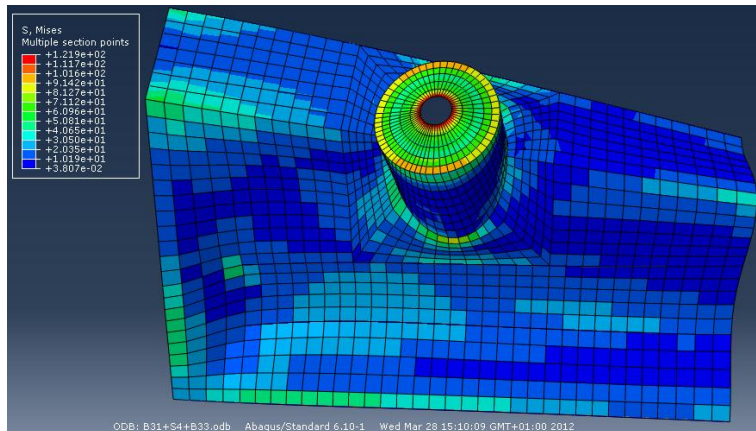


Figure 69 - VM stress for 3rd case study (Free Wing + Flange & Web Stiffeners) using B31 & S4 & B33

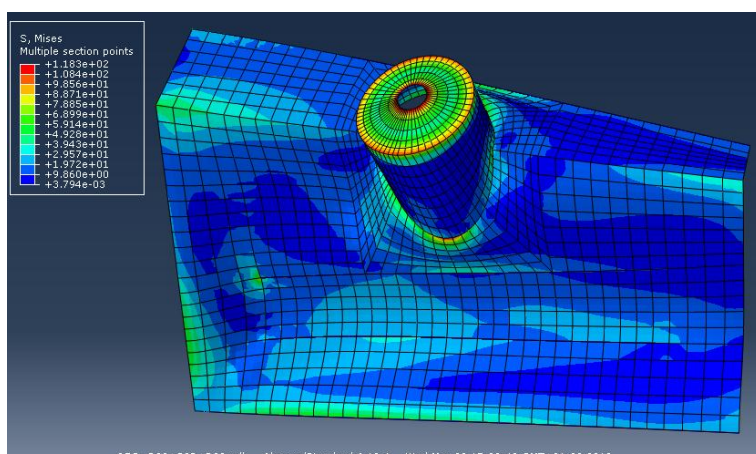


Figure 70 - VM stress for 3rd case study (Free Wing + Flange & Web Stiffeners) using B32 & S8R & B32

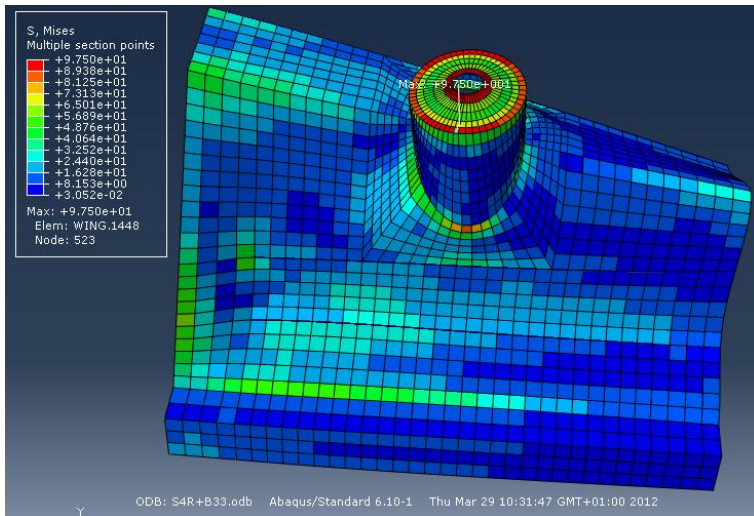


Figure 71 - VM stress for 3rd case study (Free Wing + Flange & Web Stiffeners) using S4R & B32

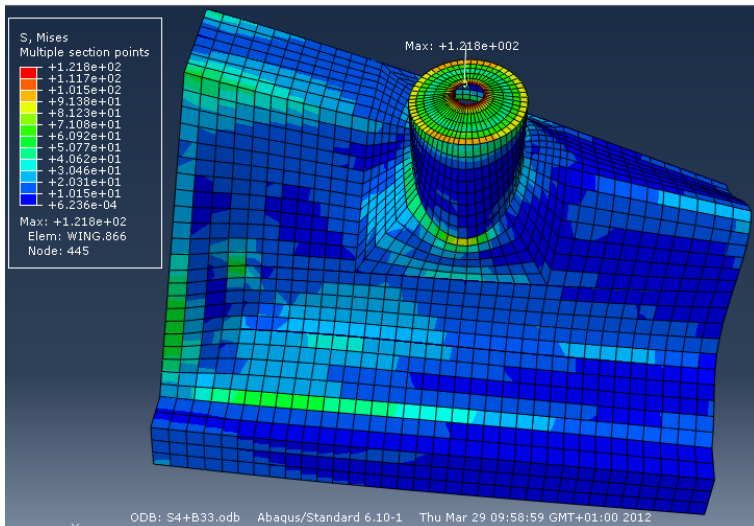


Figure 72 - VM stress for 3rd case study (Free Wing + Flange & Web Stiffeners) using S4 & B32

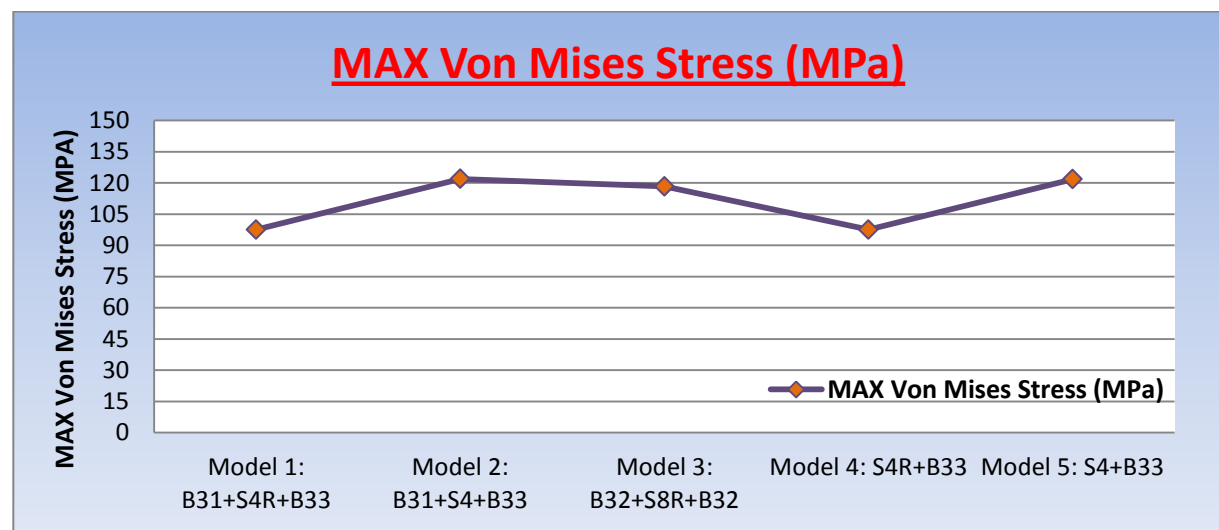


Figure 73 - Maximum Von-Mises stress evolution for the 3^d case study (Free Wing + Flange & Web stiffeners)

B. Displacements post-processing

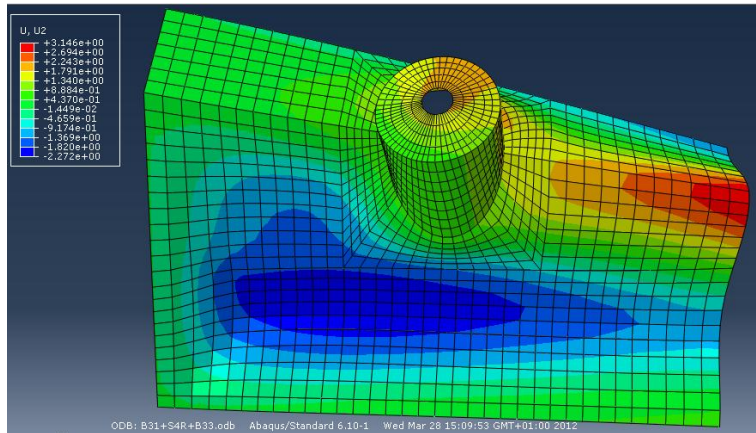


Figure 74 - Displacements for 3rd case study (Free Wing + Flange & Web Stiffeners) using B31 & S4R & B33

Observations:

- The maximum deflection is 3.146 mm and converges to 3.1 mm.
- Looking at the pictures, it has again been noticed that the amount of deflection is not reduced by the stiffeners.
- The maxima are still located at the junction of the flange and web on the free edge.

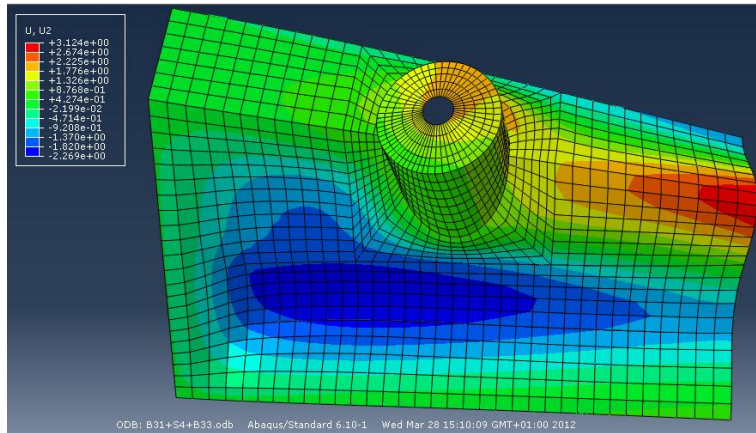


Figure 75 - Displacements for 3rd case study (Free Wing + Flange & Web Stiffeners) using B31 & S4 & B33

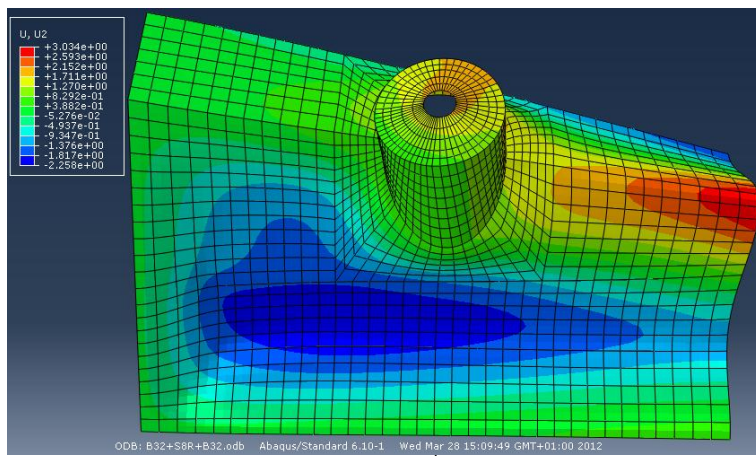


Figure 76 - Displacements for 3rd case study (Free Wing + Flange & Web Stiffeners) using B32 & S8R & B32

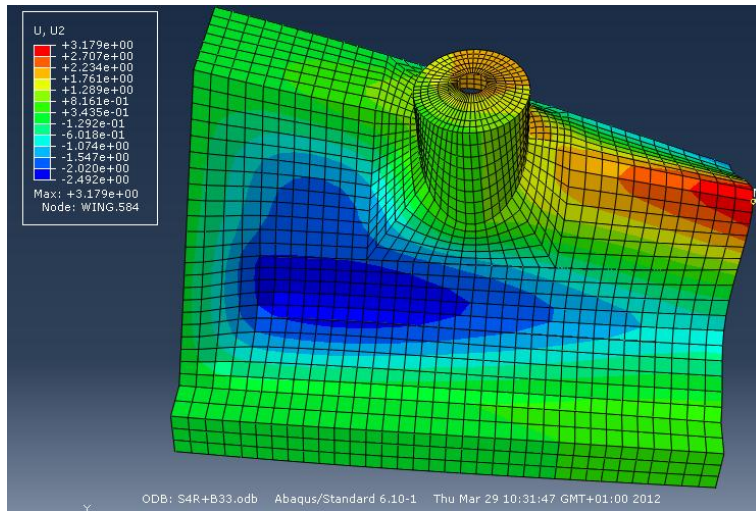


Figure 77 - Displacements for 3rd case study (Free Wing + Flange & Web Stiffeners) using S4R & B33

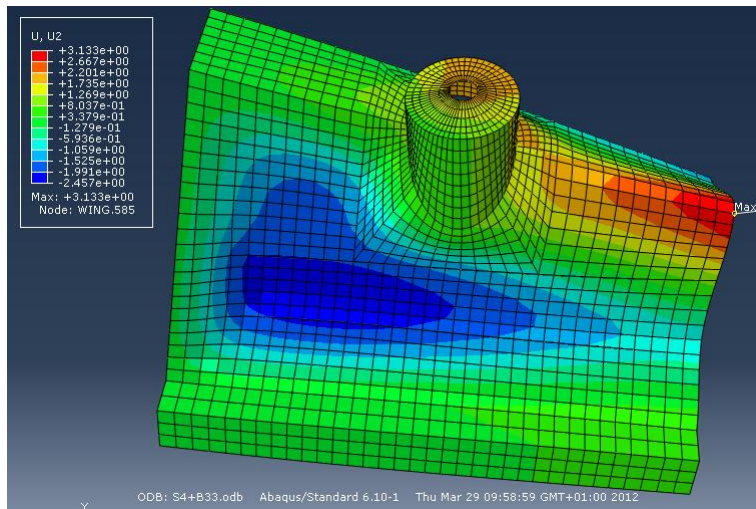


Figure 78 - Displacements for 3rd case study (Free Wing + Flange & Web Stiffeners) using S4 & B33

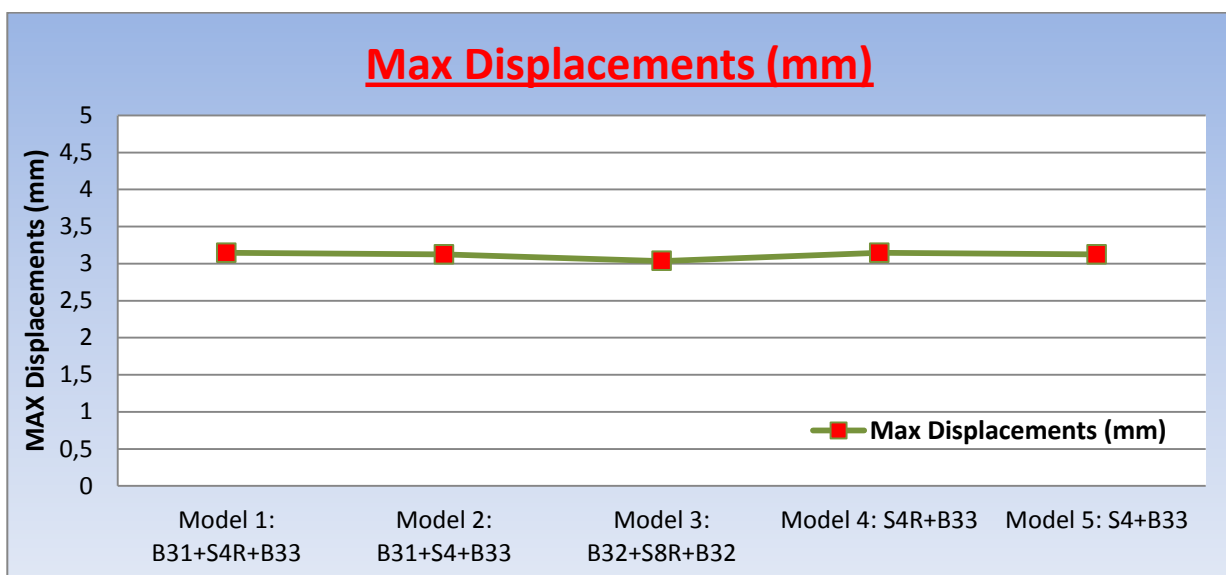
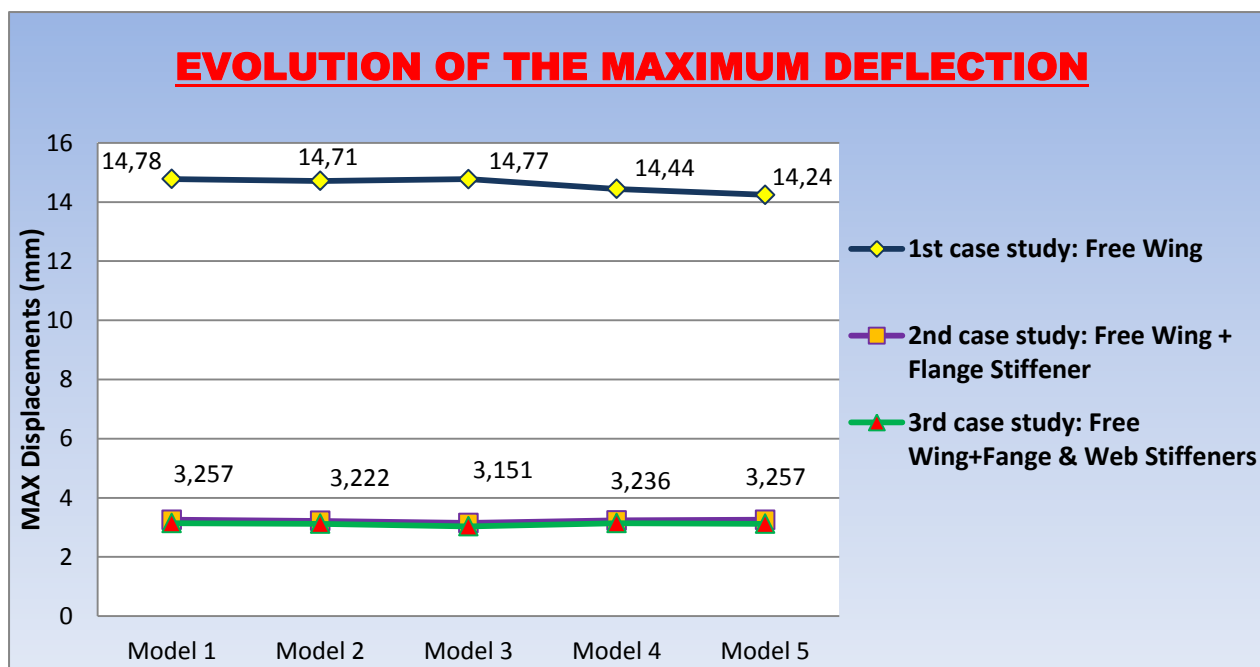
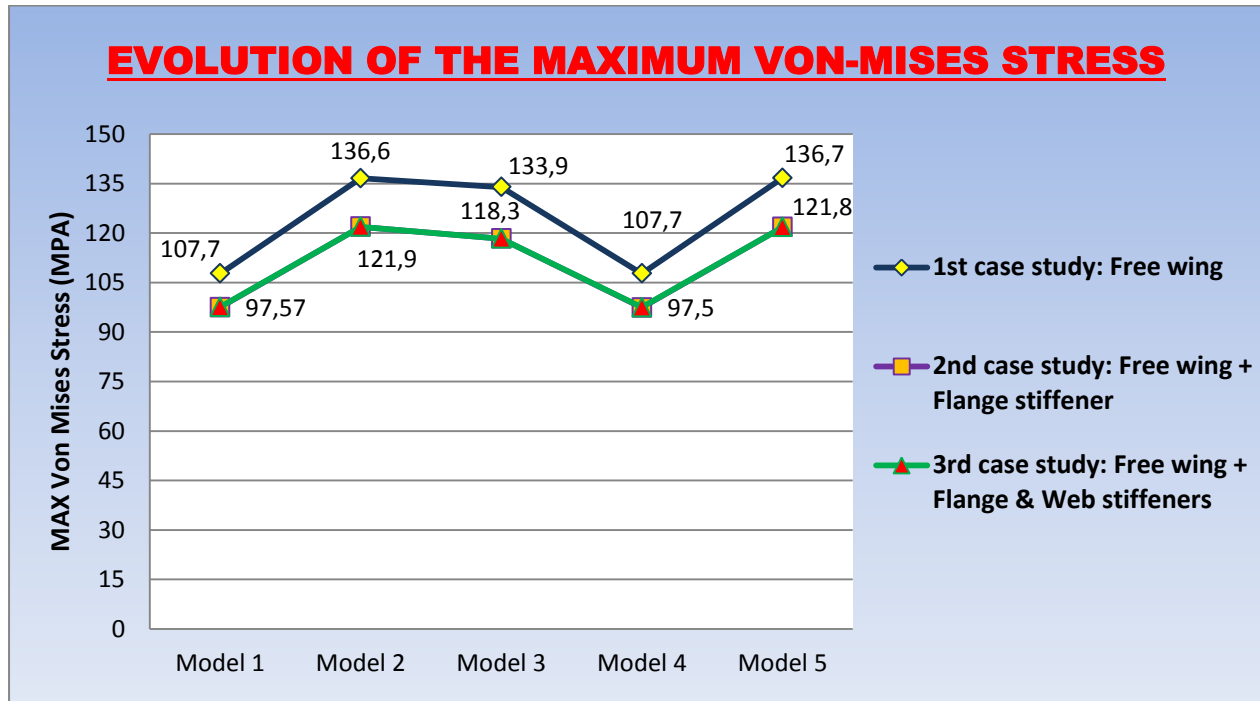


Figure 79 - Maximum Deflection evolution for the 3rd case study (Free Wing + Flange & Web stiffeners)

VII. Conclusion



Thanks to both graphics above we can notice that the first improvement, one stiffener under the flange, improve the response significantly. It allows the structure to remain in the elastic domain. However, the first case study is not relevant since the elastic yield has been exceeded. Furthermore, the third design (web stiffeners) was definitely useless since neither the stress distribution nor the deflection has been reduced. Therefore the second model could be the final single wing assembly since it respects the mechanical constraints and is cheaper than the third one.